JOURNAL OF GEOPHYSICAL RESEARCH, VOL. 104, NO. C9, PAGES 21,195–21,215, SEPTEMBER 15, 1999

Tracer distributions and deep circulation in the western tropical Atlantic during CITHER 1 and ETAMBOT cruises, 1993-1996

Chantal Andrié
Laboratoire d'Océanographie Dynamique et de Climatologie, CNRS/IRD/ Université Pierre et Marie Curie, Paris

Jean-François Ternon
Institut de Recherche pour le Développement, Cayenne, French Guiana, France

Bernard Bourlès, Yves Gouriou, and Claude Oudot
Institut de Recherche pour le Développement, Plouzané, France

Abstract. This paper presents CFC and nontransient tracer observations in the western equatorial Atlantic Ocean on repeated sections along 7°30'N, the 35°W meridian, and a transect crossing the Ceara Rise. Three World Ocean Circulation Experiment cruises have been carried out in this area, in February-March 1993 (CITHER 1) and September-October 1995 and April-May 1996 (ETAMBOT 1 and 2). Together with the tracer data, the direct current measurements are used to deduce the circulation pathways. The data confirm the principal circulation features of the Upper North Atlantic Deep Water within the area. The Deep Western Boundary Current flows southward along the continental slope, while, adjacent to the DWBC, there is a northward flow corresponding to the DWBC recirculation whose origin appears variable. The largest variability is observed along the 35°W meridional section, where the DWBC bifurcates eastward north of 3°S but the eastward equatorial flow does not appear to be permanent. At the Middle North Atlantic Deep Water level, CFC distributions exhibit the most important contrast between waters of northern and southern origin. The circulation at the Lower North Atlantic Deep Water level, mainly controlled by the topography, looks more permanent because the DWBC is regularly observed during the three cruises, and there is no evidence for a northwestward recirculation along the Mid-Atlantic Ridge. The transient behavior of CFC distributions, which is superimposed on local circulation effects, can be seen clearly through their temporal evolution within the DWBC. The variability of the deep circulation observed during the 1993-1996 interval rules out a dominant variability in response to semi annual forcing.

1. Introduction

The fate of the Deep Western Boundary Current (DWBC) at the equator is of fundamental importance for the South Atlantic water and heat budgets. The path of the DWBC, which flows southward along the American continental margin, is complicated by recirculations of the main flow, and by their associated variability. Direct velocity measurements have pointed out the complexity of the deep circulation in the western tropical Atlantic [*Johns et al.*, 1993; *Schott et al.*, 1993; *Colin et al.*, 1994; *Hall et al.*, 1997; *Fischer and Schott*, 1997]. *McCartney* [1993] has reported a wide, recirculated current spreading over the eastern part of the Guiana Basin from geostrophic calculations; *Friedrichs and Hall* [1993] and *Friedrichs et al.* [1994] have specified a cyclonic recirculation pattern in the eastern part of the Guiana Basin. CFCs [*Weiss et al.*, 1985] and SOFAR floats [*Richardson and Schmitz*, 1993; *Richardson and Fratantoni*, 1999] have shown that zonal flows exist at depth along the equator.

Chlorofluorocarbon (CFC) distributions have been extensively used to study the circulation of the DWBC within the subtropics and tropics [*Weiss et al.*, 1985; *Fine and Molinari*, 1988; *Molinari et al.*, 1992; *Pickart*, 1992; *Smethie*, 1993; *Rhein et al.*, 1995, 1998b; *Pickart et al.*, 1996]. Two North Atlantic Deep Water (NADW) components, the Upper NADW (UNADW) and the Lower NADW (LNADW), are characterized by CFC maxima located around 1600 and 3800 m respectively in the tropics, which are the signatures of their recent formation from Nordic seas, through wintertime convection processes.

Paper number 1999JC900094.
0148-0227/99/1999JC900094$09.00

Transient tracers are particularly appropriate to track the flow of the NADW, within the DWBC, from deep convective formation areas and its variability on decadal timescales [*Dickson et al.*, 1990; *Spall*, 1996; *Bönisch et al.*, 1997; *Dickson*, 1997; *Sy et al.*, 1997; *Pickart et al.*, 1997; *Vaughan and Molinari*, 1997; *Curry et al.*, 1998; *Molinari et al.*, 1998; *Pickart and Smethie*, 1998]. Questions relative to the deep circulation variability in the tropics have been addressed during several recent cruises that include tracer measurements: *Meteor* cruises from 1990 to 1994 [*Rhein et al.*, 1995, 1998b; *Plähn and Rhein*, 1998], CITHER 1 experiment in 1993 [*Andrié*, 1996; *Arhan et al.*, 1998; *Andrié et al.*, 1998; *Oudot et al.*, 1998] and ETAMBOT cruises in 1995 and 1996 [*Andrié et al.*, 1997; *Gouriou et al.*, this issue; *Oudot et al.*, this issue].

One of the goals of the ETAMBOT and the CITHER 1 experiments is to study the deep circulation variability within the western tropical Atlantic. In addition to the analysis of CFC distributions, nontransient tracers (salinity, silicate, and oxygen) help to clarify the origin of the water masses and to dissociate the temporal variability due to the local circulation from that resulting from the transient behavior of CFCs. The comparison of transient tracer distributions (such as CFCs) and nontransient tracer distributions together with direct current measurements makes it possible to partly dissociate the large-scale variability of the deep circulation from the small-scale features.

After a brief description of the measurement techniques (section 2), we present the CFC, salinity, silicate, and oxygen distributions along the sections of the CITHER 1 and ETAMBOT cruises and give the evolution of CFC-11 distributions within deep water masses (NADW) from February 1993 to May 1996 (section 3). We then present, for the ETAMBOT 2 cruise, the simultaneous horizontal current and CFC-11 distributions in order to propose circulation schemes at the UNADW and LNADW levels (section 4). Finally, we discuss the variability over different time periods of the deep circulation as inferred through the CFC-11 distributions and earlier studies (section 5).

2. Data Sets and Methods

The CITHER 1 (CIT1) cruise took place in January-March 1993 [*Arhan et al.*, 1998; *Andrié et al.*, 1998; *Oudot et al.*, 1998] and consisted of two trans-Atlantic sections along 4°30'S (World Ocean Circulation Experiment (WOCE) A7) and 7°30'N (WOCE A6) linked at 35°W and 4°W by two meridional sections. As a continuation of CITHER 1, the main objective of the ETAMBOT program was to focus on the study of equatorial circulation within the western basin, between the American continent and the Mid-Atlantic Ridge (MAR). The two ETAMBOT cruises took place during two seasons: ETAMBOT 1 (ET1) in September-October 1995 and ETAMBOT 2 (ET2) in April-May 1996. The ETAMBOT cruise track (Figure 1) reoccupies the CIT1 sections along the 7°30'N latitude (between the French Guiana coast and 35°W) and along the 35°W longitude (from 7°30'N to 5°S). During both ETAMBOT cruises, a third section crossed the Ceara Rise, off Brazil. This section is referred to as the "Ceara section." In this paper, we discuss only the CIT1 data for the area west of the 35°W section (Figure 1).

The principal topographic features in the region shown in Figure 1 are the Demerara Rise between 9°30'N and 7°N (see the shape of the 2000-m isobath), the Ceara Rise between 6°N and 3°N (45°W-40°W) (delimited by the 4000-m isobath contour), and the equatorial channel limited to the south by the Parnaiba Ridge and to the north by the MAR (Figure 1).

Conductivity-temperature-depth-oxygen ($CTDO_2$) measurements were carried out during the three cruises with a Neil Brown MARK III. Precision of sensors and reproducibility of the measurements are discussed in data reports [*Groupe CITHER 1*, 1994; *Equipe ETAMBOT*, 1997a, b] and by *Bourlès et al.* [this issue]. During CIT1 an 8-L, 32-bottle rosette was used. During the ETAMBOT cruises, 22 bottles were installed on an 8-L, 24-bottle General Oceanics rosette; double casts were performed when the bottom depth exceeded 4500 m, in which case, 28 levels were sampled. Below 1000 m depth the vertical sampling resolution was similar for the three cruises (see Figure 2a) and the horizontal station interval was between 20 nautical miles (37 km) at the equator and near the topographic structures and 30 nautical miles (55.6 km) (see *Andrié et al.* [1998] for CIT1), corresponding to the WOCE recommendations.

The measurement errors for bottle salinity and bottle oxygen are less than 0.001 and 0.5 μmol kg^{-1}, respectively. The analytical precision for silicate, determined from test stations and duplicate samples, is around $\pm$ 0.2 μmol kg^{-1} [see *Oudot et al.*, this issue].

The technique used for CFC measurements is the classical extraction-trapping method coupled to gas chromatography with electron capture detection [*Bullister and Weiss*, 1988]. Data calibrated using a primary standard provided by the Scripps Institution of Oceanography (SIO) (1986 scale) have been converted to the SIO 1993 scale. The standard analytical precisions including (1) the use of a secondary atmospheric standard for routine analyses, (2) reproducibility for standard injections, and (3) determination of a fitted calibration curve, are within 1% for both CFC-11 and CFC-12.

A blank determination method is reported for CIT1 by *Andrié et al.* [1998]. Deviations between measured CFC contents of sea surface samples and theoretical concentrations corresponding to solubility equilibrium with the atmosphere [*Warner and Weiss*, 1985] are close to the detection limit and similar for the three cruises. The respective "blank" background and detection limit of the analytical methods for each cruise are given in Table 1. Owing to the withdrawal of a specific mean blank value for each cruise, for the whole data set, CFC-11 (and even more, CFC-12) data comparisons between all three cruises have to be considered with caution for the lowest concentrations (e.g., < 0.02 pmol kg^{-1}). To avoid redundancy, we report here only data relative to the more soluble CFC-11 compound (hereinafter referred to as CFC).

During the ETAMBOT cruises, direct current measurements were made over the whole water column with a lowered acoustic Doppler current profiler (LADCP) attached to the rosette. Thirty-three LADCP velocity profiles were obtained along the 7°30'N latitude during ET1, while during ET2, LADCP profiles were obtained at almost all the stations [*Equipe ETAMBOT*, 1997a, b]. Complementary details on the quality of the LADCP measurements are given by *Gouriou et al.* [this issue].

3. Tracer Distributions From 1993 to 1996

Owing to their different boundary conditions, the CFCs, salinity, and silicate tracers can be used to specify the respective northern (CFC and salinity maxima, silicate

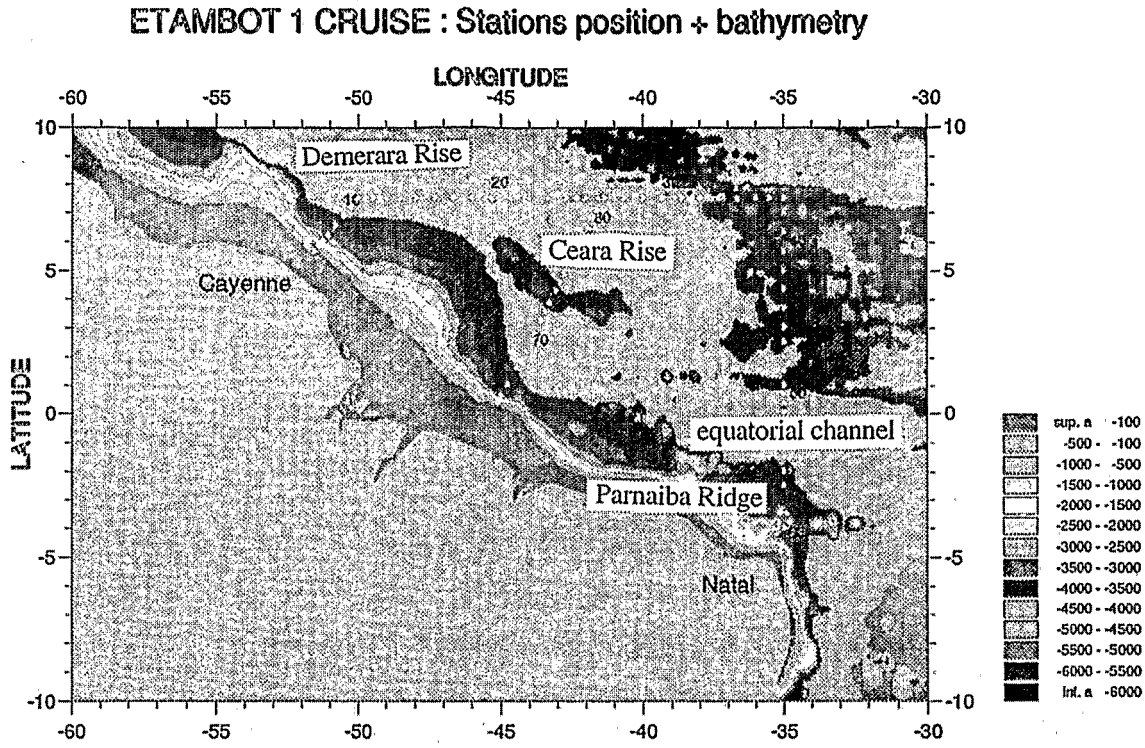

Figure 1. Station locations of the ETAMBOT 1 cruise (April-May 1996). The bottom topography shows the Demerara Rise, the Ceara Rise, and the equatorial channel, to the north of the Parnaiba Ridge. The three sampled transects are the zonal 7°30'N section, the slanted Ceara section, and the meridian 35°W section.

minima) or southern (CFC minima, silicate maxima) origins of the deep water masses. Considering the high correlation observed, for each cruise, between CFCs, salinity, and silicate, we report here only the nontransient tracer distributions relative to the ET2 cruise. When comparing the cruises, the differences in the geographical distribution of the CFCs and of the nontransient tracers emphasize the transient behavior of the CFCs. This CFC transient behavior can reflect the aging of the water masses or the variability of the ventilation processes at high latitude.

Figures 2 to 7 show tracer distributions for CIT1, ET1 and ET2 along three sections (see Figure 1), respectively, the 7°30'N section (Figures 2a, 3a, 4a, 5a, 6a, and 7a), the 35°W section (Figures 2b, 3b, 4b, 5b , 6b, and 7b), the Ceara section (Figures 3c, 4c, 5c, 6c, and 7c) (only for ET1 and ET2).

The CFC minima observed around 1000 m depth (Figures 2, 3, and 4) correspond to the Upper Circumpolar Water (UCPW), just below the Antarctic Intermediate Water (AAIW). They are characterized by a salinity minimum and silicate maximum (Figures 5 and 6). Below 1000 m the two tongues of CFC maxima are clearly visible around 1500-1800 and 3800-3900 m and correspond to the UNADW and LNADW, respectively. Both cores of CFCs are known to be transported southward within the DWBC [*Weiss et al.*, 1985; *Fine and Molinari*, 1988; *Molinari et al.*, 1992; *Rhein et al.*, 1995, 1998b; *Andrié et al.*, 1998].

The northward flowing Antarctic Bottom Water (AABW) lies above the bottom, as a mixture of Weddell Sea Bottom Water (WSBW) and Lower Circumpolar Water (LCPW). Whereas the WSBW is a recently ventilated water and characterized with the presence of CFCs, the LCPW is mainly characterized by CFC-free waters, a potential temperature minimum, and a silicate maximum (Figure 6) as described by *Rhein et al.* [1998a].

3.1. UNADW

Formation of the upper core of NADW occurs mainly during the boreal winter in the southern Labrador Sea [*Pickart*, 1992]. During its southward transport this water mass mixes with Gulf Stream waters [*Pickart*, 1992; *Spall*, 1996] and then with the Mediterranean Water (MW) through recirculation cells and eddies [*Reid*, 1994; *Curry et al.*, 1998]. In the subtropics and tropics the CFC maximum is associated with a salinity maximum characterizing the MW (Figure 5a) and corresponds to the shallow UNADW [*Pickart*, 1992; *Pickart et al.*, 1996, 1997]. *Rhein et al.* [1995] find that the UNADW lies at a potential temperature between 3.4°C and 4.5°, density $\sigma_{1.5}$ between 34.42 and 34.70, and depth between 1200 and 1900 m.

The UNADW is marked by a silicate minimum (Figure 6a) contrasting with the overlying and silicate-enriched UCPW [*Oudot et al.*, 1998, this issue]. The UNADW is distinct from the underlying Labrador Sea Water (LSW) (the upper part of the Middle NADW), and there is no oxygen maximum (Figure 7a) associated with the CFC maximum [*Rhein et al.*, 1995]. Although CFC and oxygen both enter the ocean in high latitudes through ventilation processes, their distributions are very different at the UNADW level (Figures 2a, 3a, 4a, and 7a). Within the tropics the apparent oxygen utilization rate is the highest around 800-1000 m, at the same depth as the silicate maximum [*Oudot et al.*, 1998], and this large oxygen consumption erodes the oxygen maximum down to 1600 m.

Table 1. Mean Blank Level and Detection Limit of the Analytical Method for CFC-11 and CFC-12 for the Three Cruises

	CFC-11		CFC-12	
	Mean Blank Level	Detection Limit	Mean Blank Level	Detection Limit
CITHER 1	0.007-0.009	0.0025	0.002-0.006	0.0025
ETAMBOT 1	0.007-0.033	0.01	0.002	0.004
ETAMBOT 2	0.025	0.008	0.003	0.005

Values are in pmol kg^{-1}.

Several CFC maxima are observed all along the 7°30'N section from the western boundary to 35°W (Figures 2a, 3a, and 4a). Within this tongue the CFC cores mirror perfectly the salinity maxima (Figure 5a) and silicate minima (Figure 6a). On the western boundary of the 7°30'N section the tracer maxima correspond to the UNADW carried directly within the DWBC southward. The CFC cores (>0.2 pmol kg^{-1} for CIT1 and >0.35 pmol kg^{-1} for ET1 and ET2) correspond to salinity exceeding 35.000. The eastern edge of these cores has been described as a possible recirculation of the DWBC [*Molinari et al.*, 1992; *McCartney*, 1993; *Richardson and Schmitz*, 1993; *Colin et al.*, 1994; *Schott et al.*, 1993; *Fischer and Schott*, 1997; *Andrié et al.*, 1998]. From float trajectories at 1800 m between 11°N and 1°S, in the area to the west of 43°W, *Richardson and Fratantoni* [1999] describe a 90-km-wide DWBC and a 110-km-wide northward current corresponding to the DWBC recirculation, just to the east of the direct DWBC. A thinning of the core is observed around 100 km offshore during CIT1 (Figure 2a). Such a feature was also observed in February 1989 along the "French Guiana" section by *Molinari et al.* [1992], probably as the result of an extremely narrow DWBC not resolved by the station spacing. The similar CFC concentrations measured within both direct and recirculated DWBC during ET2 (Figures 4a and 4c) indicate that the recirculation occurs from an area close to the Ceara section. This result provides new information on the previously reported equatorial velocity fields, which do not describe any recirculation to the west of the Ceara Rise [*Friedrichs and Hall*, 1993; *Friedrichs et al.*, 1994; *Molinari et al.*, 1992; *Rhein et al.*, 1995, 1998b; *Fischer and Schott*, 1997].

A particular feature is observed during ET2 around 50°W along the 7°30'N section, where low CFC (Figure 4a), low salinity (Figure 5a), and high silicate (Figure 6a) concentrations reflect a mesoscale gyre structure. The observed deepening of salinity and CFC isolines support an associated vertical intrusion of overlying UCPW waters.

Other maxima of tracer concentrations are observed at various longitudes offshore (Figures 2a, 3a, and 4a). *Andrié et al.* [1998] attribute these maxima to either northern inputs or a recirculation of the DWBC along the western flank of the MAR.

Despite their same general structure along 7°30'N, the CFC distributions differ from CIT1 (March 1993) to ET1 (September 1995) and ET2 (April 1996) (Figures 2a, 3a, and 4a). As expected and contrary to the distributions of salinity and silicate, the transient behavior of CFCs is clearly evidenced along 7°30'N, particularly during the 2.5 years between CIT1 and ET1.

Along the Ceara section, during ET1 and ET2, three CFC-enriched structures are found (Figures 3c and 4c): close to the continental margin (with an offshore extension to 4°N for ET2), at 5°N (just north of the Ceara Rise), and around 7°N. During ET2 the CFC-11 maximum (mean concentration > 0.22 pmol kg^{-1}, Figure 4c), spreading to 500 km offshore, has properties similar to the northeastern extension of the CFC-11 core observed at the same distance from the DWBC along the 7°30'N section (>0.34 pmol kg^{-1} around 47°W, Figure 4a). The shapes of the salinity and silicate structures (Figures 5c and 6c) are similar to those observed at 7°30'N (Figures 5a and 6a). The CFC-11 core found between the coastal DWBC and the Ceara Rise during ET2 (Figure 4c) can result either from a recirculating branch of the DWBC, originating from a southernmost area, or from a local mesoscale structure. During both ET1 and ET2 cruises (Figures 3c, 4c, 5c, and 6c), CFC minima are observed above the Ceara Rise (4°30'N-1600 m) associated with a salinity minimum and a silicate maximum (less marked for ET1 than for ET2).

On the 35°W section the CFC distributions of the three cruises exhibit considerable differences (Figures 2b, 3b, and 4b) that are caused by the circulation pattern [*Rhein et al.*, 1995, 1998b; *Fischer and Schott*, 1997]. The three enriched structures observed on both sides of the equator during CIT1 (Figure 2b) are also observed during ET1 (Figure 3b): one CFC-enriched core extending from the southern boundary to 500 km offshore, south of the equator; CFC lenses, not permanent, from the equator to 3°N; and CFC cores between 4°N and 6°N. For ET1 these cores seem to correspond to the structures observed upstream on the Ceara section (Figure 4c). During ET2 the CFC distribution is asymmetric north and south of the equator (Figure 4b), unlike during CIT1 and ET1 (Figures 2b and 3b). On the southern edge of the 35°W section the CFC concentrations did not increase between ET1 and ET2. Moreover, the minimum around 1800 m, south and north of the equator (Figure 4b), is more extended than for ET1 (Figure 3b). A well-defined CFC lens is observed at the equator at 1500 m during ET2, also well evidenced as a silicate minimum (<16 µmol kg^{-1}, Figure 6b), which is associated with a deep equatorial jet [see *Gouriou et al.*, this issue]. One of the most striking features observed during ET2 is the large CFC core located between 4°N and 7°N (Figure 4b) around 1500 m depth. At 6°20'N the CFC core (0.28 pmol kg^{-1}) is associated with a salinity maximum (35.004) and a silicate minimum (16.3 µmol kg^{-1}), which indicate a northern origin for this water mass. The core seems to be connected to the CFC maximum observed at 7°N on the Ceara section (0.25 pmol kg^{-1} for CFC, 35.003 for salinity, 15.6 µmol kg^{-1} for silicate). A similar connection is observed in the overlying UCPW in silicate concentrations [*Oudot et al.*, this issue]. Somewhat different tracer properties are observed to the east of the 7°30'N section (0.14 pmol kg^{-1} for CFC, 34.989 for salinity, 18.4 µmol kg^{-1} for silicate at 35°30'W).

For the three cruises we observe a continuous decrease of CFC concentrations from 7°30'N to the Ceara section and to 35°W. During CIT1 and partly during ET2 the absence of any strong CFC maximum on the southern edge of the 35°W section can be related to the bottom topography steering the DWBC pathway up to 1500 m depth and particularly to the

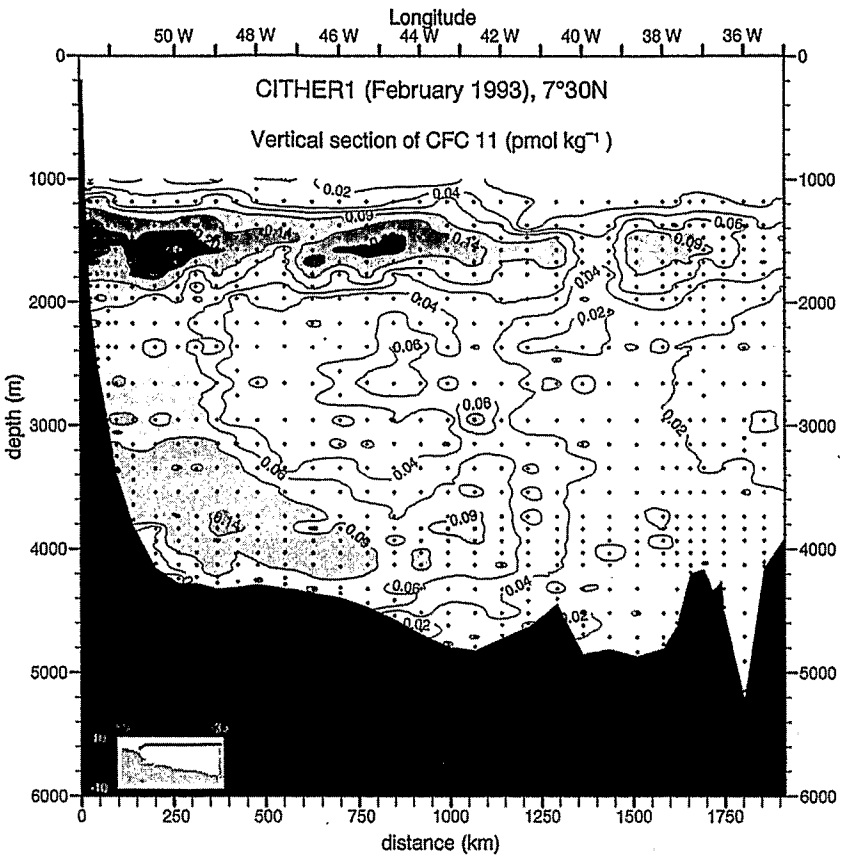

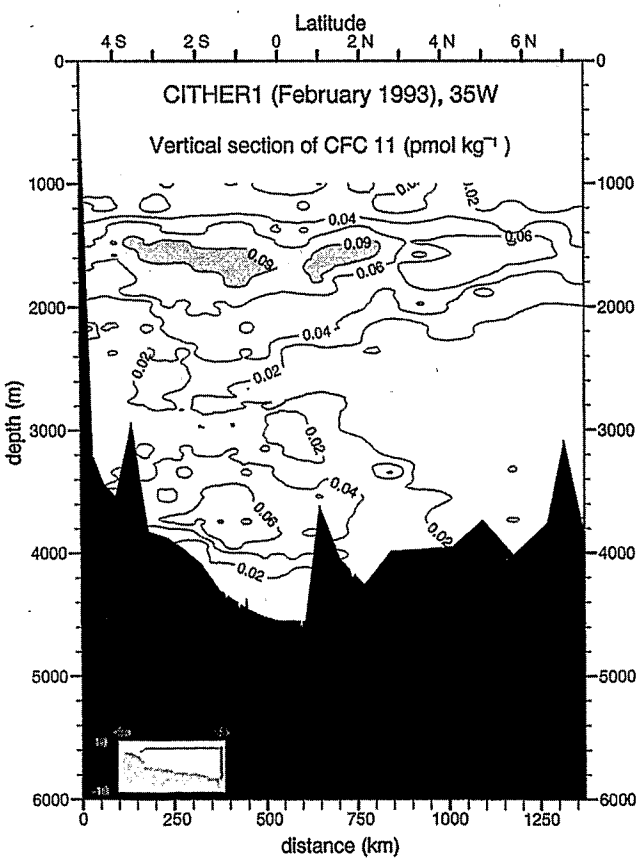

Figure 2. Vertical sections of CFC-11 (pmol kg^{-1}) obtained during CITHER 1 (CIT1) in February-March 1993 along the transects shown in Figure 1. (a) The 7°30'N section (with dots corresponding to the sampled levels). A similar sampling strategy has been used during the three cruises and along the three transects. (b) The 35°W section (Ceara section has not been sampled for CIT1).

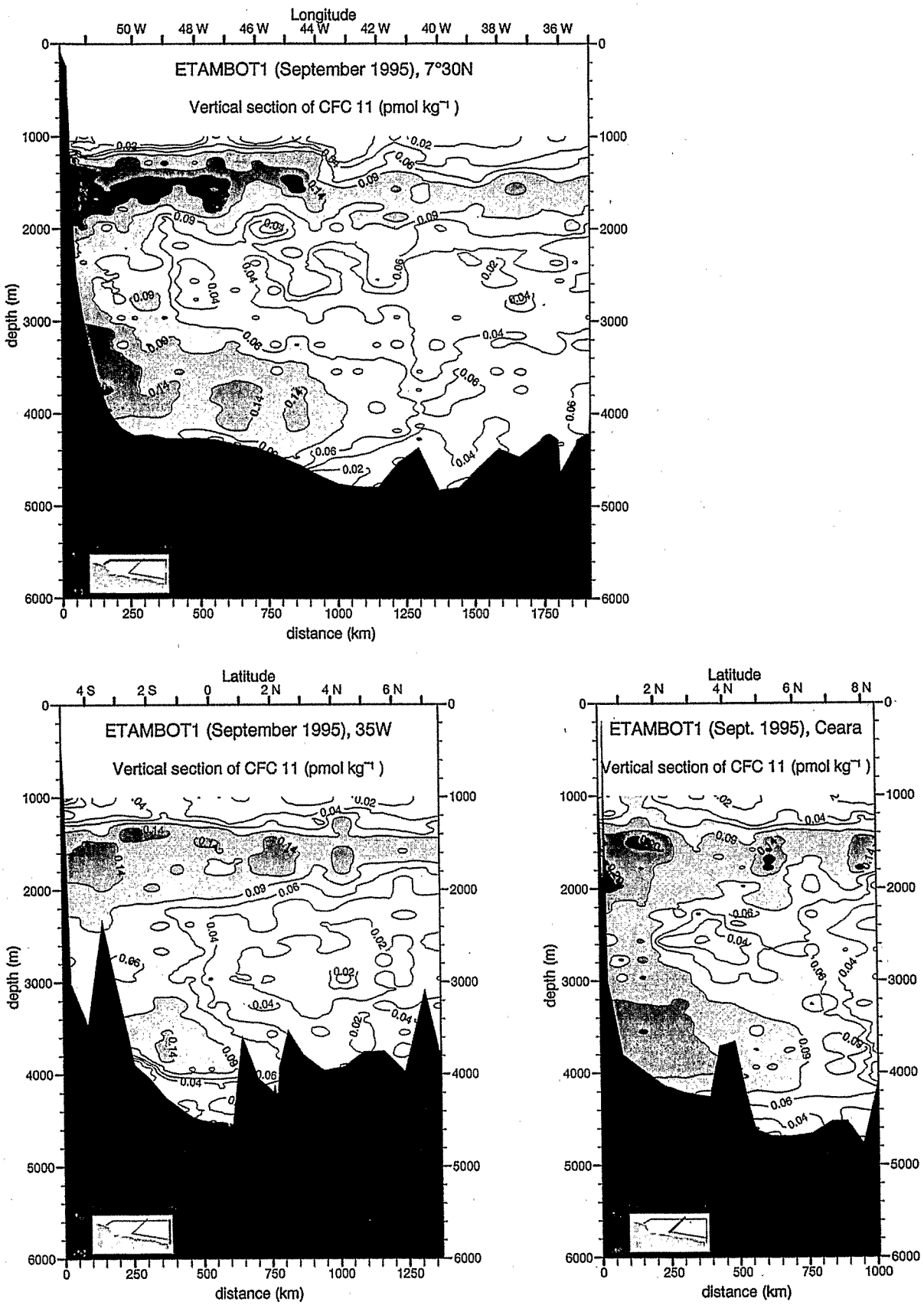

Figure 3. Vertical sections of CFC-11 (pmol kg^{-1}) obtained during ETAMBOT 1 (ET1) in September-October 1995 along the (a) 7°30'N, (b) 35°W and (c) Ceara sections.

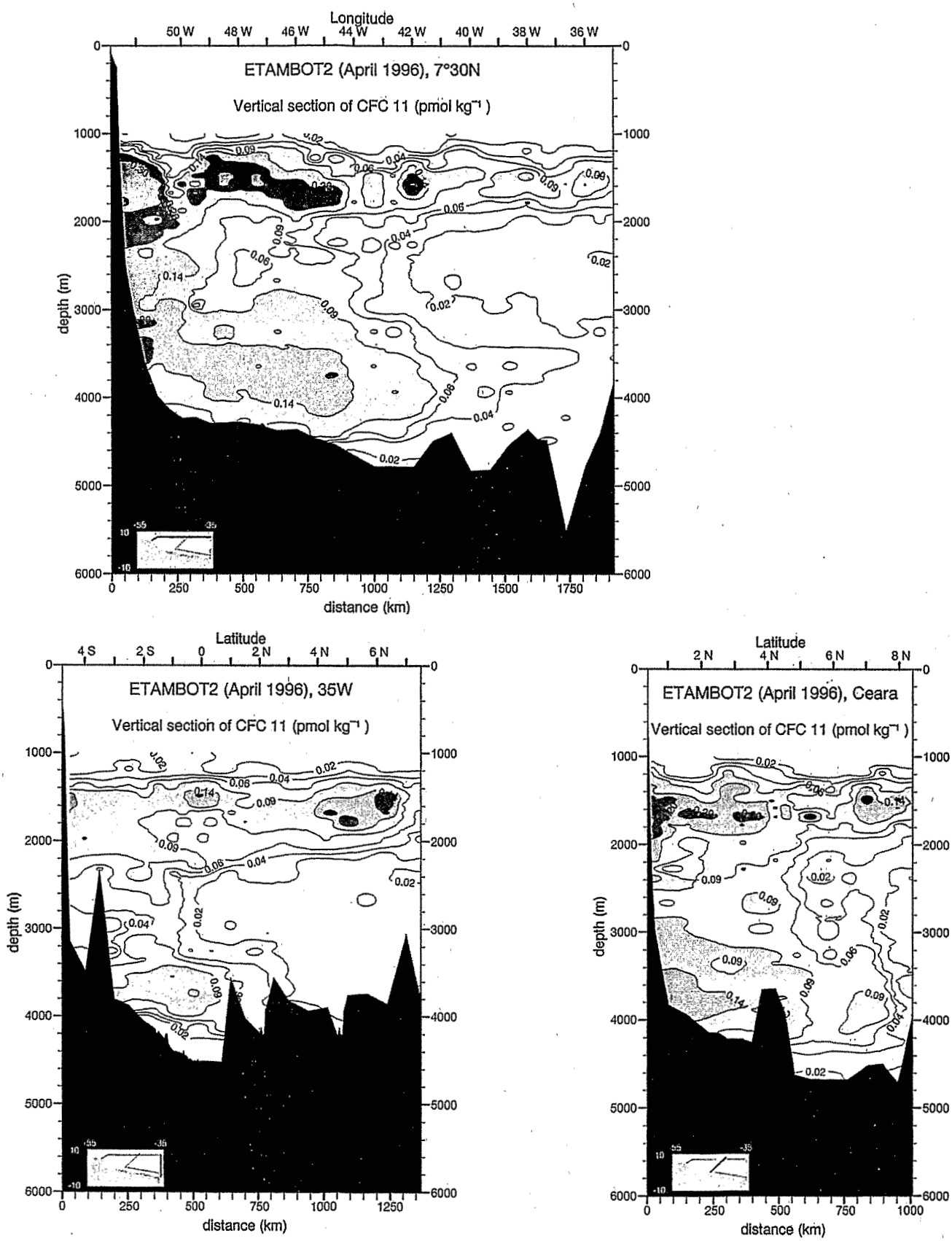

Figure 4. Vertical sections of CFC-11 (pmol kg^{-1}) obtained during ETAMBOT 2 (ET2) in April-May 1996 along the (a) 7°30'N, (b) 35°W and (c) Ceara sections.

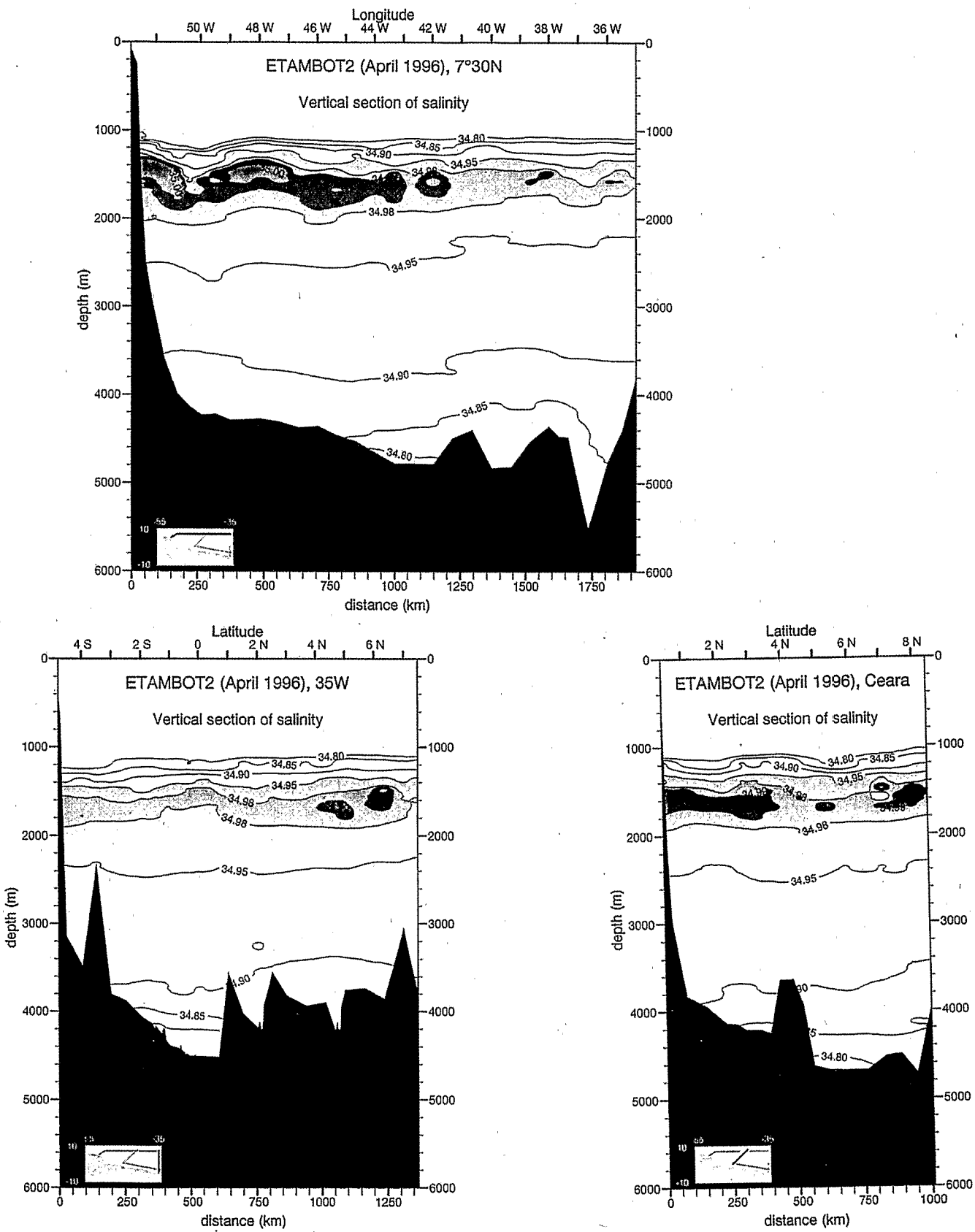

Figure 5. Vertical sections of salinity obtained during ETAMBOT 2 in April-May 1996 along the (a) 7°30'N, (b) 35°W and (c) Ceara sections.

presence of seamounts near 3°30'S, causing recirculation of the DWBC flow as discussed by *Fischer and Schott* [1997] and *Richardson and Fratantoni* [1999]. The similarity between CFCs, salinity, and silicate distributions emphasizes the importance of the variability of local circulation.

3.2. MNADW

The MNADW is characterized by a CFC minimum, sandwiched between the CFC cores of the UNADW and LNADW (Figures 2, 3, and 4). It lies between 2000 and 3000 m (mean σ_2 = 37.03). In the upper part of the MNADW (around 1900-2400 m) the LSW component is identified through its high oxygen content. The oxygen enrichment extends vertically from 2000 m to the bottom (Figure 7a). This vertical increasing trend is due to the temperature effect on solubility. The observed oxygen distribution results from an integration process over successive periods of intense/weak convection events within the Labrador Sea. Conversely, for transient tracers such as CFCs, weak convection occurring during the 1960s and 1970s [*Lazier*, 1988; *Rhein et al.*, 1995; *Pickart et al.*, 1997; *Curry et al.*, 1998] together with the absence of man-made CFCs before the 1940-1950s, explain that no CFC signal was detected below 2000 m in the western deep Atlantic south of Barbados before 1995 [*Molinari et al.*, 1998; *Pickart and Smethie*, 1998].

The underlying water mass below the LSW is referred to by *Rhein et al.* [1995] as the lower "old" NADW, characterized by low oxygen and low CFC concentrations. It is mainly composed of Gibbs Fracture Zone Water (GFZW) and southern Circumpolar Water (CPW) [*Reid*, 1994; *Talley and Johnson*, 1994]. Owing to the transient origin of CFCs and the particular history of the water mass, the most striking differences between CFC and other tracer distributions are observed on the MNADW level.

A CFC enrichment is observed within the DWBC from 1993 to 1996 on the western side of the 7°30'N section to about 350 km offshore between 2000 and 3500 m (Figures 2a, 3a, and 4a). For each cruise, similar oxygen structures are observed at 2600 m depth, around 50°W and 46°W (Figure 7a for ET2). At 7°30'W we observe a CFC minimum around 3000 m depth at 49°30'W for each cruise (Figures 2a, 3a, and 4a), corresponding to an input of a low-oxygen, high-silicate water mass. Such a structure corresponds to poorly ventilated, southern origin water, sandwiched between southward flowing waters [*McCartney*, 1993; *Andrié et al.*, 1998].

Similar to the UNADW level along 7°30'N, the eastward extension of the CFC tongue within the DWBC varies between the three cruises: the 0.06 pmol kg^{-1} isoline at 49°W for CIT1 (and ET1) has been shifted eastward to 44°W for ET2. For the three cruises we observe CFC cores in the middle of the Guiana basin around 45°W at 7°30'N and around 4°N-5°N across the Ceara section (> 0.06 pmol kg^{-1}), centered at about 2600 m depth (Figures 2a, 3a, and 4a, and 3c and 4c). For CIT1 and ET2 these maxima are associated with "chimney-like" structures also observed for oxygen sections (Figure 7a). These structures could be due to mixing with the underlying LNADW through diffusion or upwelling. From CIT1 data and an inverse model, M. Lux et al. (Interhemispheric exchanges of mass and heat in the Atlantic Ocean in January-March 1993, submitted to *J. Geophys. Res.*, 1999) have identified a diapycnal transfer of LNADW into MNADW. Nevertheless, little is known about the reasons and location of such vertical advection.

The CFC distributions observed along the Ceara section during ET1 and ET2 (Figures 3c and 4c) exhibit a front between CFC-enriched and low-CFC waters, just east of the Ceara Rise (around 750 km offshore for ET1 and 500 km offshore for ET2). The CFC minimum is particularly well marked during ET2, at 6°N (700 km offshore), centered around 2400-2700 m. Such a front was observed along 7°30'N (Figures 3a and 4a), somewhat shifted offshore during ET2. On the ET1 Ceara section (Figure 3c) the CFC minimum at 8°N is less pronounced than for ET2 (Figure 4c) and there is no CFC minimum around 5°-6°N. On the other hand, there is a wide CFC minimum (< 0.04 pmol kg^{-1}) around 4°N, above the Ceara Rise, corresponding to high silicate concentration (>30 µmol kg^{-1}, not shown).

On the 35°W section (Figures 2b, 3b, and 4b), around 3000 m, we observe a vertical front in the middle of the equatorial channel with low-CFC water to the north and higher CFC concentrations to the south, with minima surrounding the Parnaiba Ridge around 3000 m. These minima probably mark the center of a recirculation as described by *Andrié et al.* [1998] for CIT1.

3.3. LNADW

The LNADW (or overflow LNADW after *Rhein et al.* [1995]) is a mixture of water masses formed by convection from the surface, north of the Greenland-Scotland sills and upstream of the Denmark Strait [*Smethie et al.*, 1986; *Schlosser et al.*, 1991; *Rhein*, 1991, 1996; *Mauritzen*, 1996; *Döscher and Redler*, 1997]. *Rhein et al.* [1995] report a potential temperature of LNADW in the sampled area between 1.75°C and 2.2°C for a density σ_4 between 45.83 and 45.90 (mean σ_3 = 41.50), which corresponds to a depth around 3500-3900 m. The LNADW is characterized by an oxygen maximum (Figure 7). There are no particular features of salinity and silicate distributions at this level (Figures 5 and 6) owing to very similar distributions of this property within LNADW and surrounding water masses. A relative silicate minimum characterizes the LNADW [*Oudot et al.*, 1998].

The LNADW is coincident with high CFCs in the west of the 7°30'N section, on the southern edge of the Ceara section, and on the 35°W section (Figures 2, 3, and 4). The CFC distributions are essentially constrained by the topography. The 0.06 pmol kg^{-1} isoline does not extend eastward of 41°W for the three cruises along 7°30'N, as the result of topographic blockings due to seamounts in the east and the Ceara Rise in the south [*Plähn and Rhein*, 1998, *Rhein et al.*, 1998b].

High CFC concentrations (> 0.10 pmol kg^{-1}) are observed offshore of the 4000-m isobath along the Ceara and 35°W sections (Figures 3c and 4c). The associated oxygen distribution (Figure 7 for ET2) shows identical structures. A silicate (and phosphate, not shown) increase at the eastern boundary of the LNADW tongue also shows the offshore limit of the LNADW tongue [*Oudot et al.*, 1998]. CFC concentrations are generally lower northeast than southwest of the Ceara Rise. This suggests that the preferential pathway for the LNADW is located on the southwestern flank of the Ceara Rise. During ET2 we observe around 8°N, between 3500 and 4000 m, a northeastward rising of the silicate isolines

(Figure 6c) associated with sharp CFC and oxygen gradients which were also noticeable between 40°W and 42°W along the 7°30'N section (Figures 4a and 7a). The observed silicate concentrations result from the input of high- silicate waters originating from the Southern Hemisphere along the western flank of the MAR. The associated low CFC concentration rules out a DWBC recirculation along the MAR as suggested by *McCartney* [1993] and *Friedrichs et al.* [1994] and discussed by *Plähn and Rhein* [1998].

At 35°W, CFC and oxygen cores are observed in the middle of the equatorial channel (Figures 2b, 3b, 4b, and 7b). They result from the DWBC eastward bifurcation (2°S-0°30'N), essentially induced by the topography [*Rhein et al.*, 1995, 1998b; *Hall et al.*, 1997; *Fischer and Schott*, 1997; *Andrié et al.*, 1998; *Arhan et al.*, 1998]. North of the northern ridge of the equatorial channel, CFC concentrations are close to the detection limit. To the east toward the Romanche Fracture Zone, the LNADW core has been described as a permanent feature of the equatorial circulation [*Speer and McCartney*, 1991; *Mercier et al.*, 1994; *Messias et al.*, 1999; Direct observations of low frequency fluctuations in the deep equatorial Atlantic ocean, V.Thierry et al., submitted to *J. Geophys. Res.*, 1999].

The largest temporal increase in CFC concentration inside the LNADW core occurred between ET1 and ET2 along the 7°30'N section (Figures 2a, 3a, and 4a). The eastward progression of the 0.14 pmol kg^{-1} isoline can be clearly observed from 1993 to 1996 (mainly between 1995 and 1996). Within the equatorial channel the maximum CFC concentration of the LNADW increases from CIT1 to ET1 and ET2, in agreement with the increase described by *Rhein et al.* [1998b] between 1990 and 1994.

4. Circulation Patterns

4.1. Circulation Patterns During ETAMBOT 2, April-May 1996

In Plates 1a-1c, we interpret the CFC distributions during ET2 together with the velocity measurements along the three sections. At the UNADW level (σ_2=36.88), Plate 1a shows the progressive decrease of the CFC concentrations from the 7°30'N section to the south of the 35°W section within the southward flowing DWBC, trapped along the American continental margin. Within the DWBC, CFC maxima correspond to the maximum southeastward velocities. The previously described minimum CFC concentration observed at 50°W (Figure 4a) could correspond to the center of an anticyclonic gyre and/or to a shear between two horizontal currents: a northward current (centered around 50°30'W) and a southward current (centered around 49°W) (Plate 1a). The vertical gradient of CFC concentrations around 50°W (Figure 4a) indicates that mixing associated with these dynamics could result from mixing low-CFC UCPW downward, and could lead to low CFC concentration in the upper part of the UNADW. Such structures have been observed by *Richardson and Fratantoni* [1999] through convoluted float trajectories as the possible result of deep vertical extension of the retroflection of the North Brazil Current (NBC). Offshore, the circulation pattern is more complex. We observe successive opposite flows corresponding to alternate enriched/poor CFC cores, possibly resulting from the meandering behavior of the DWBC recirculated eastward. This is, in particular, clearly visible through the two CFC cores observed at 49°W and 47°W along 7°30'N (Plate 1a), associated with maximum opposite velocities. The somewhat greater CFC concentration observed at 47°W than at 49°W could be the result of two superimposed CFC inputs consisting of an eastward meandering flow and/or a northward input from the southwest of the Ceara Rise. West of the Ceara Rise, we observe a strong northwestward flow centered on 2°-3°N, associated with enriched CFC waters (Figure 4b). This feature can result either from a DWBC recirculation originating from a southern area or from a local mesoscale structure.

On the 35°W section the DWBC bifurcates eastward at 5°S as a very narrow DWBC, trapped against the coast and characterized by moderately enriched CFC waters compared to the Ceara and 7°30'N sections. This CFC concentration decrease confirms the assumption that the northward (and/or eastward) recirculation of the DWBC during ET2 takes place upstream of the 35°W meridian, probably very close to the Ceara Rise. To the north of the equator we observe weak currents, mainly southward, associated with low CFC concentrations. The low velocity corresponding to the CFC core observed around 5°N-6°N at 35°W does not confirm the northern origin of the structure that was inferred from tracer distributions (section 3).

Velocity structure is less organized in the northeastern part of the ETAMBOT triangle than in the southeast (Plate 1a), similar to the CFC distribution (Figures 4a-4c). Possible eastward meandering flow seems to be present along the 7°30'N section, associated with a decrease in the CFC concentration. A horizontal shear in current distribution is observed above the Ceara Rise (4°N), which coincides with a CFC minimum. North of this, a mean southeastward flow is observed together with one isolated CFC core around 5°N. However, from the velocity field, there is no sign of any recirculation to the north of the Ceara Rise.

From the whole ET2 velocity pattern there is no evidence of a permanent recirculation flow in the Guiana Basin, between the Ceara Rise and the MAR, as suggested by *McCartney* [1993] and *Friedrichs and Hall* [1993]. On the other hand, just along the western side of the MAR (at 39°W-40°W), an isolated southeastward flow, associated with low CFC concentration, could correspond to the circulation feature described along the MAR by *Friedrichs and Hall* [1993].

At the MNADW level (Plate 1b), across the 7°30'N and the Ceara sections, the southeastward flowing DWBC is visible east of the continental slope and somewhat shifted offshore across the 35°W section at 1°30'S. This DWBC flow is associated with a high-CFC concentration core. The southeastward velocity within the DWBC is lower (<10 cm s^{-1}) than at the UNADW level (>30 cm s^{-1}) (Plate 1a). Continuity of the DWBC flow and the associated high CFC concentration between 7°30'N, the Ceara, and the 35°W sections is not as clear as that for the UNADW level. The flow pattern has a south-north asymmetry, with high southeastward flow on the western edge of the 7°30'N section and to the south of the Ceara Rise and eastward flow within the equatorial channel. It is difficult to identify clearly a northwestward flow core along the western side of the MAR [*Friedrichs and Hall*, 1993; *Friedrichs et al.*, 1994].

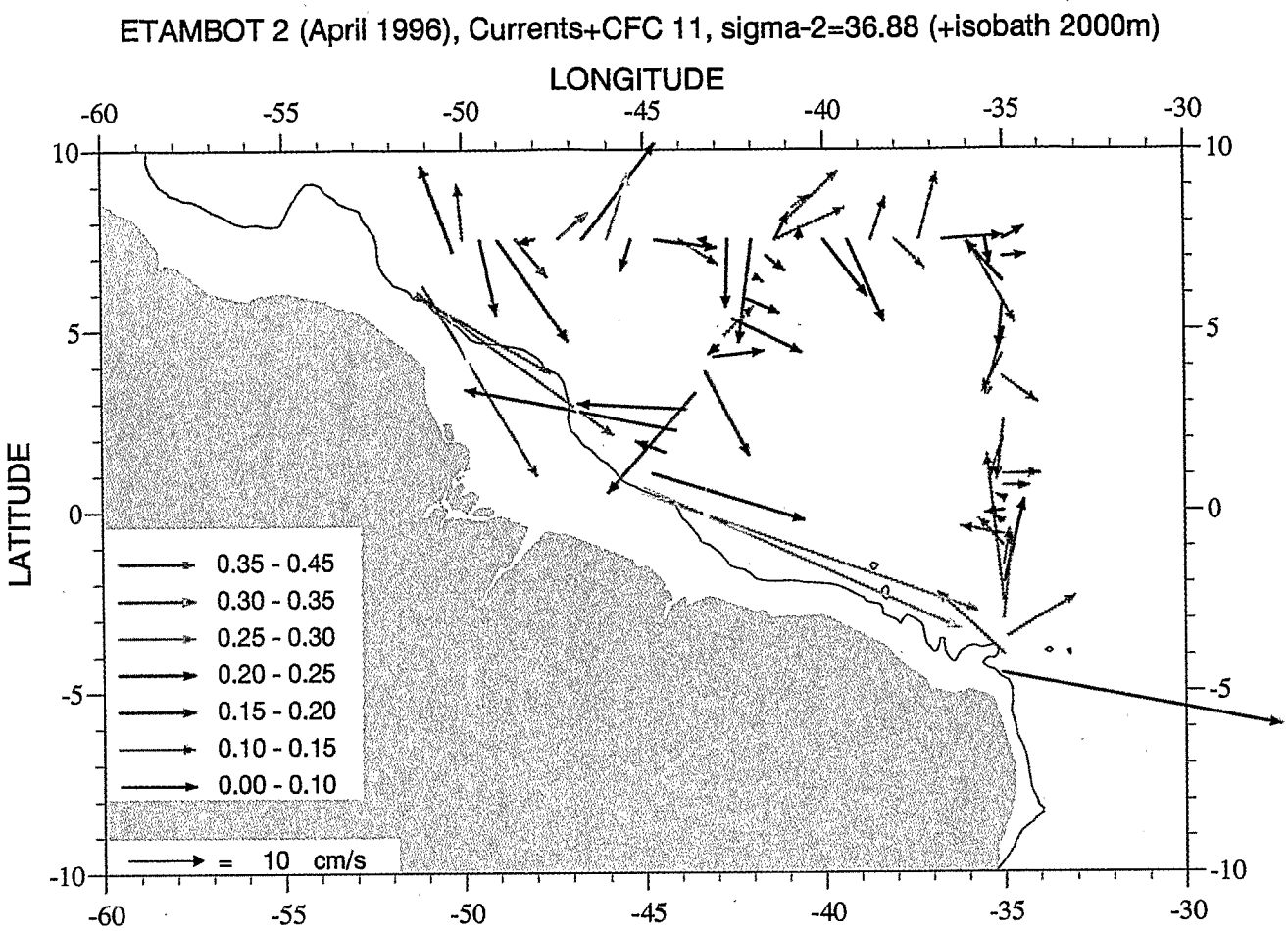

Plate 1a. Horizontal velocity distributions from lowered acoustic Doppler current profiler measurements during ETAMBOT 2 at the upper North Atlantic Deep Water level (σ_2=36.88). The CFC-11 concentrations (following the color legend) are superimposed on the vector currents (in cm s^{-1}).

At the LNADW level (Plate 1c) the DWBC core is still observed on the western side of the 7°30'N section, against the continental slope and associated with high CFC concentrations. Several isolated northward flows are observed from east of the DWBC to 44°W, associated with high CFCs. The shape of the 4000-m isobath (Plate 1c) explains how the Ceara Rise blocks and deviates the LNADW to the north (as recirculated pathways) or to the east. A branch of the LNADW flows directly southeastward through the deep strait located between the continental slope and the Ceara Rise. Then, the Parnaiba Ridge (on the southern edge of the equatorial channel, at 2°S, see Figure 1) forces the LNADW to flow eastward.

In the middle of the eastern Guiana Basin a continuous southeastward flow is observed from 43°W-7°30'N and around 6°N, to the northeast of the Ceara Rise. This flow corresponds to a CFC minimum. This is in contradiction with the assumption of *Friedrichs et al.* [1994], discussed by *Plähn and Rhein* [1998], who present arguments for a northward recirculation along the MAR at the LNADW level. In addition, there is no northwestward current identified (Plate 1c) along the MAR (excepted at the equator).

The 35°W section exhibits a strong eastward current around 1°30'S, to the south of the equatorial channel, associated with high CFC concentrations. This flow is a permanent feature of the deep circulation, as it was observed on the repeated section of the *Meteor* cruises [*Rhein et al.*, 1995, 1998b; *Plähn and Rhein*, 1998] and through continuous measurements from moorings at 35°W [*Hall et al.*, 1997; *Fischer and Schott*, 1997]. The westward component observed near the northern ridge of the equatorial channel (at 0°20'N) could be the signature of a DWBC recirculation. However, the current distribution in the northern part of the Ceara does not show any CFC-enriched northwestward flow during ET2 that could confirm this assumption.

4.2. General Circulation Schemes

Friedrichs and Hall [1993], *Friedrichs et al.*[1994], and *Rhein et al.* [1995] have suggested circulation patterns for the UNADW, MNADW, and LNADW layers that have been discussed partly by *Andrié et al.* [1998]. Some different circulation features have been inferred from the 1993-1996 data set. The circulation inferred from the CIT1, ET1, and ET2 tracer distributions and ET2 current measurements at the UNADW level corresponds to the following general patterns: (1) A CFC-enriched DWBC flows southward, trapped along the continental slope. (2) Adjacent to the DWBC, a CFC-enriched northward flow was observed during CIT1 and ET2 and absent

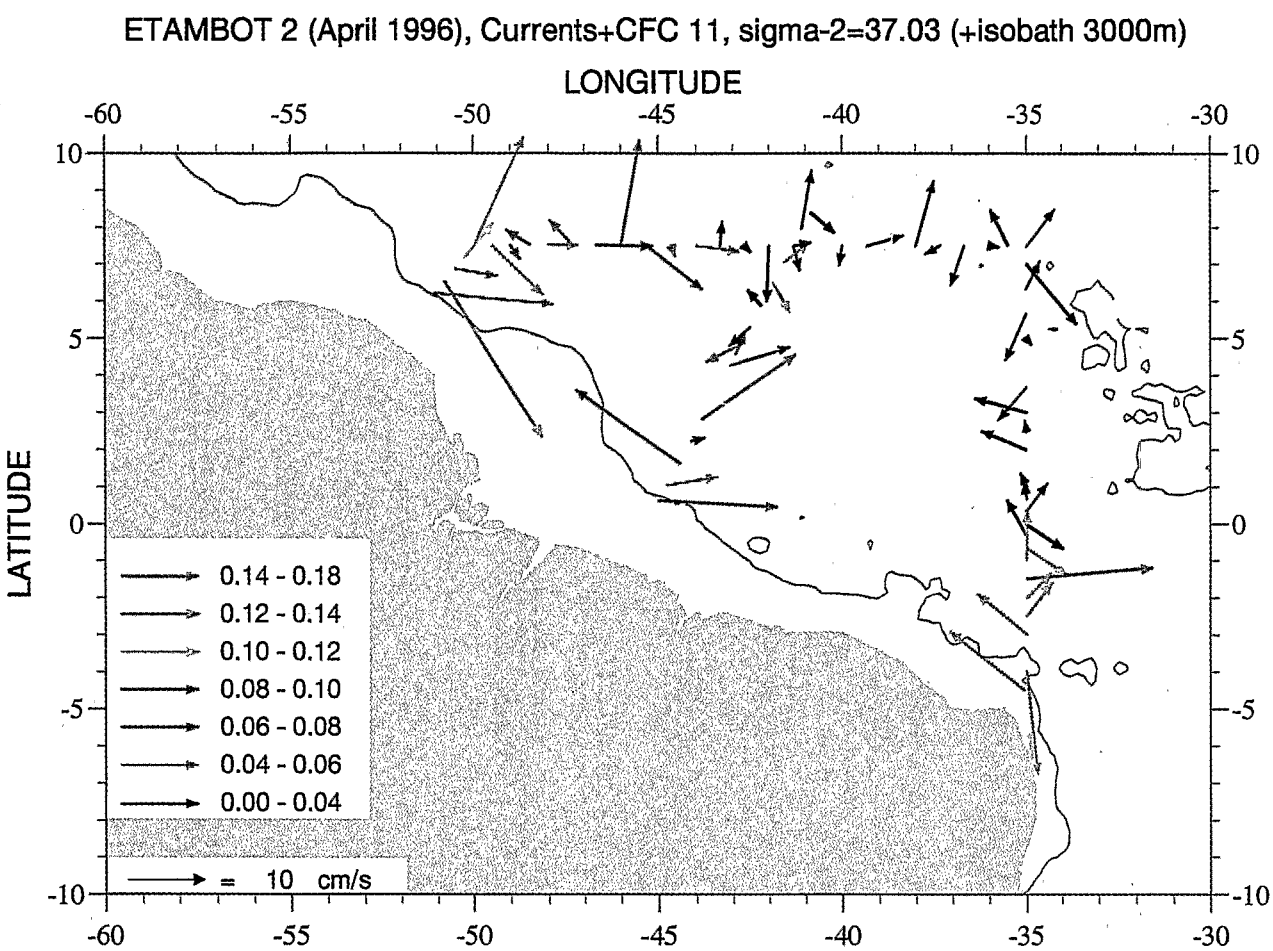

Plate 1b. Same as Plate 1a but at the middle North Atlantic Deep Water level (σ_2 = 37.03).

during ET1. This feature, due to a northward DWBC recirculation, is observed on both 7°30'N and Ceara sections. (3) The CFC distributions suggest that the northward recirculation of the DWBC originates from at least two areas: the first offshore and north of 5°N and the second, which flows back northwestward on the western side of the Ceara Rise, upstream of the 35°W meridian. (4) There is an asymmetry east and west of the Ceara Rise. While part of the southward DWBC recirculates northward along the southern side of the Ceara Rise (feature not observed during ET1), a southward flow is observed between the Ceara Rise and the MAR, characterized by enriched CFC cores and concentrations that increase with the absolute southward velocity. Just to the south of the Ceara Rise, we observe a strong southward flow with CFC-enriched cores, turning around the rise and partly feeding the northward flow. North of the Ceara Rise, there is an area of weak flow, with low CFC concentration. (5) A southeastward flow seems to be present along the western side of the MAR, characterized by low CFC waters. (6) The largest spatiotemporal variability is observed along the 35°W meridional section. The DWBC bifurcates eastward at 1°30'S, and the equatorial flow, which reveals jet-like structures, does not seem permanent. During boreal winter and spring cruises (CIT1 and ET2) some intermittent flow from the DWBC seems to maintain a tracer core around 6°N along 35°W.

The circulation at the LNADW level is controlled by the topography and shows less temporal variability than that of the UNADW: (1) The DWBC is observed during the three cruises, with CFC concentrations half of those observed at the UNADW level. (2) The southward flowing DWBC is partly blocked north of 6°N by the topography. Part of the DWBC recirculates northward around 48°W, whereas another part flows southward. (3) The LNADW flows southward mostly on the western side of the Ceara Rise and then eastward in the south of the equatorial channel. (4) There is no evidence of a northwestward recirculation along the MAR.

The MNADW has common characteristics with the LNADW level: (1) CFC-free waters of southern origin are observed on the three 7°30'N sections in the northern part of the Guiana Basin, associated with a low mean northward flow. (2) For the three cruises, CFC and salinity minima and silicate maxima are observed around 3000 m depth, approximately 250 km offshore, along the three 7°30'N sections. These features suggest a permanent northward flow of southern waters or an area of weak flow. (3) During boreal winter and spring cruises (CIT1 and ET2) a northward recirculated flow, adjacent to the DWBC, is responsible for an eastward extension of the CFC core. Unlike the circulation pattern observed at the UNADW level, this feature is visible on the 7°30'N section but not on the Ceara section. (4) Chimney-like structures within the CFC

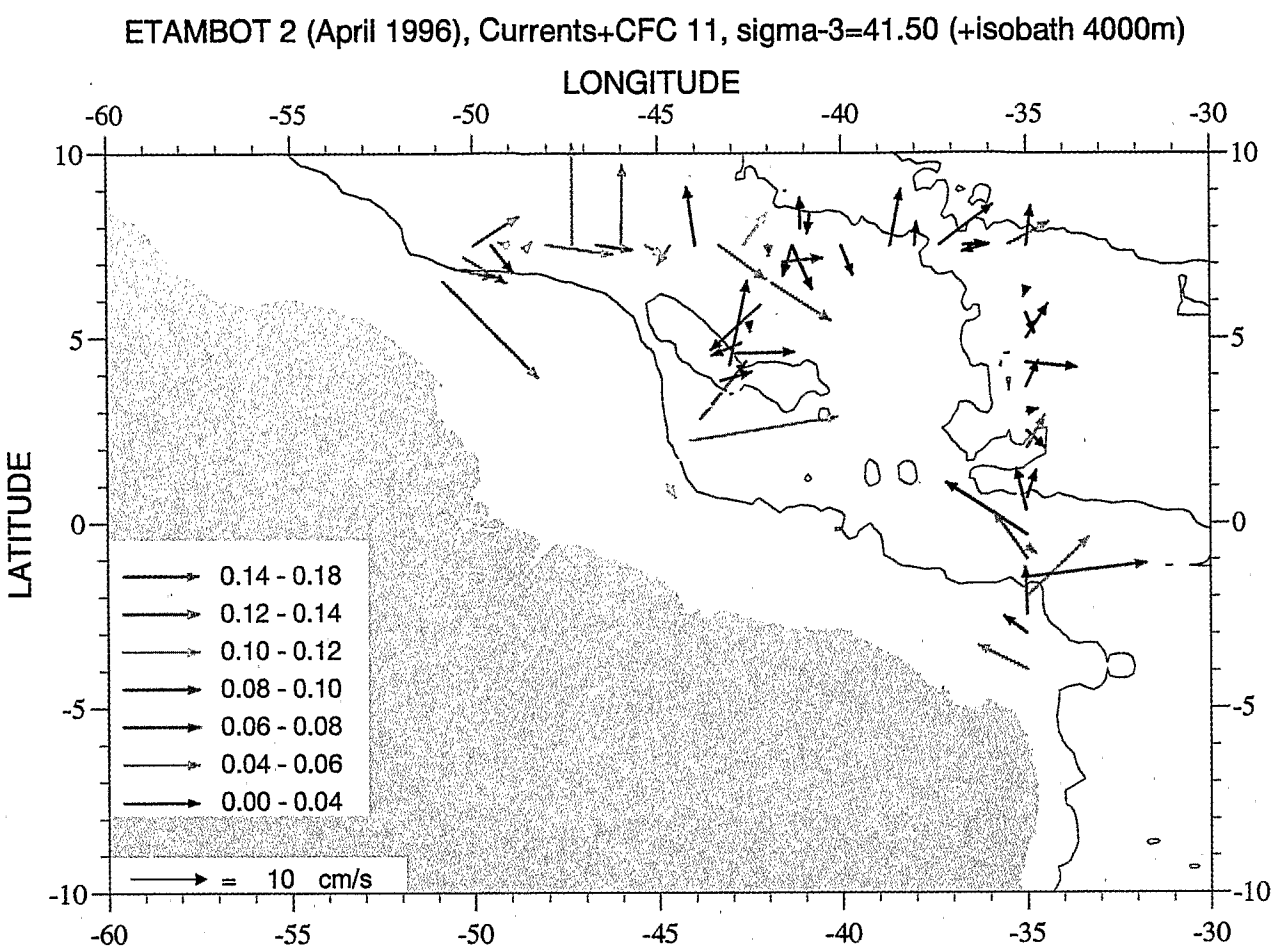

Plate 1c. Same as Plate 1a but at the lower North Atlantic Deep Water level (σ_3= 41.50).

distributions in the middle of the Guiana Basin seem to indicate mixing with the LNADW through vertical diffusion or upwelling.

5. Discussion

Different variability modes are evidenced from the temporal evolution of CFC distributions along the three sections and from the comparison with distributions of nontransient tracers such as salinity, oxygen, and silicate. The similarity between the LADCP velocity field and the CFC distributions shows that the local circulation generally dominates the tracer distributions. We discuss herein some examples of variability linked to local dynamics. Such features are superimposed on the long-term variability observed for each section through the CFC and nontransient concentrations.

5.1. Variability of the DWBC and Its Recirculation

At the UNADW level the ET2 velocity pattern (Plate 1a) differs somewhat from that of ET1 [*Andrié et al.*, 1997]. During ET2 a DWBC recirculated flow is present at the 7°30'N longitude, both to the southwest and just north of the Ceara Rise. LADCP and tracer measurements do not show such a recirculation during ET1 [*Andrié et al.*, 1997]. During ET2 the CFC core is wider (200-250 km wide, Figure 4a) and associated with a greater southward velocity of the direct DWBC within the UNADW core than during CIT1 and ET1 (100-150 km wide, Figures 2a and 3a). The width of the tracer core depends on the eastward extent of the recirculated DWBC (or its remnant) and on the velocity of the direct DWBC.

On the western side of the Ceara section a CFC core is observed, which is more enriched and wider during ET2 than during ET1 (Figures 3c and 4c). From CFC distributions it seems that recirculation was probably not present during ET1 near the Ceara.

The spatiotemporal variability of the recirculation (distance offshore, current velocity) could be linked to DWBC variability itself [*Richardson and Fratantoni*, 1999]. Mechanisms such as pulsing of the DWBC, strength, or interaction with equatorial waves linked to seasonal surface forcing can be invoked. *Pickart and Smethie* [1998] suggest a seasonally varying volume flux within the DWBC linked to a downstream pulse after each convective season with possible local response of the deeper LNADW flow to the upper flow. Several current measurement experiments have been performed in the deep tropical western Atlantic, which have identified seasonal or semiannual variability for the DWBC [*Schott et al.*, 1993; *Johns et al.*, 1993; *Lee et al.*, 1996; *Fischer and Schott*, 1997; *Hall et al.*, 1997]. Theoretical or modeling approaches reproduce similar periods when superimposing

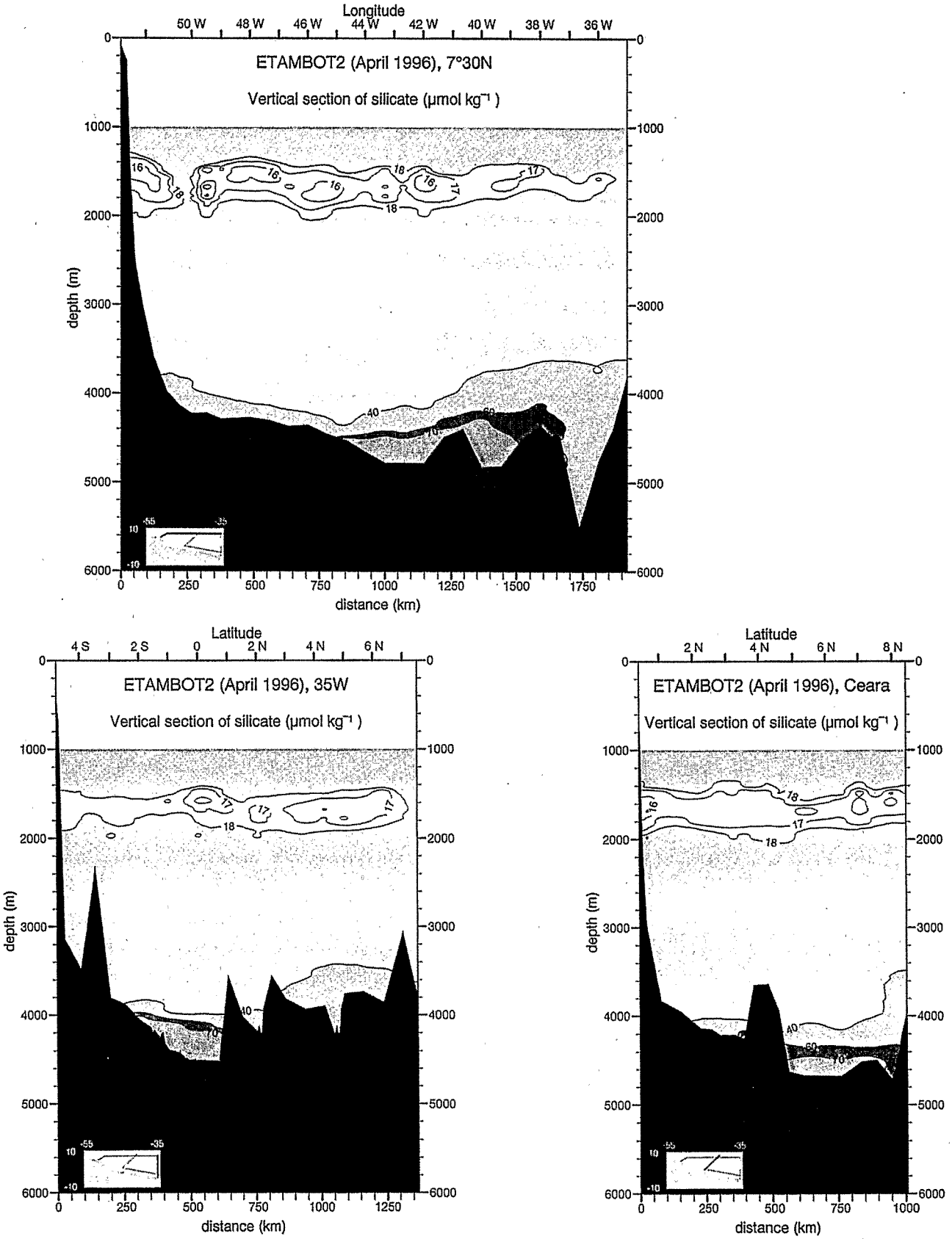

Figure 6. Vertical sections of silicate (µmol kg^{-1}) obtained during ETAMBOT 2 in April-May 1996 along the (a) 7°30'N, (b) 35°W and (c) Ceara sections.

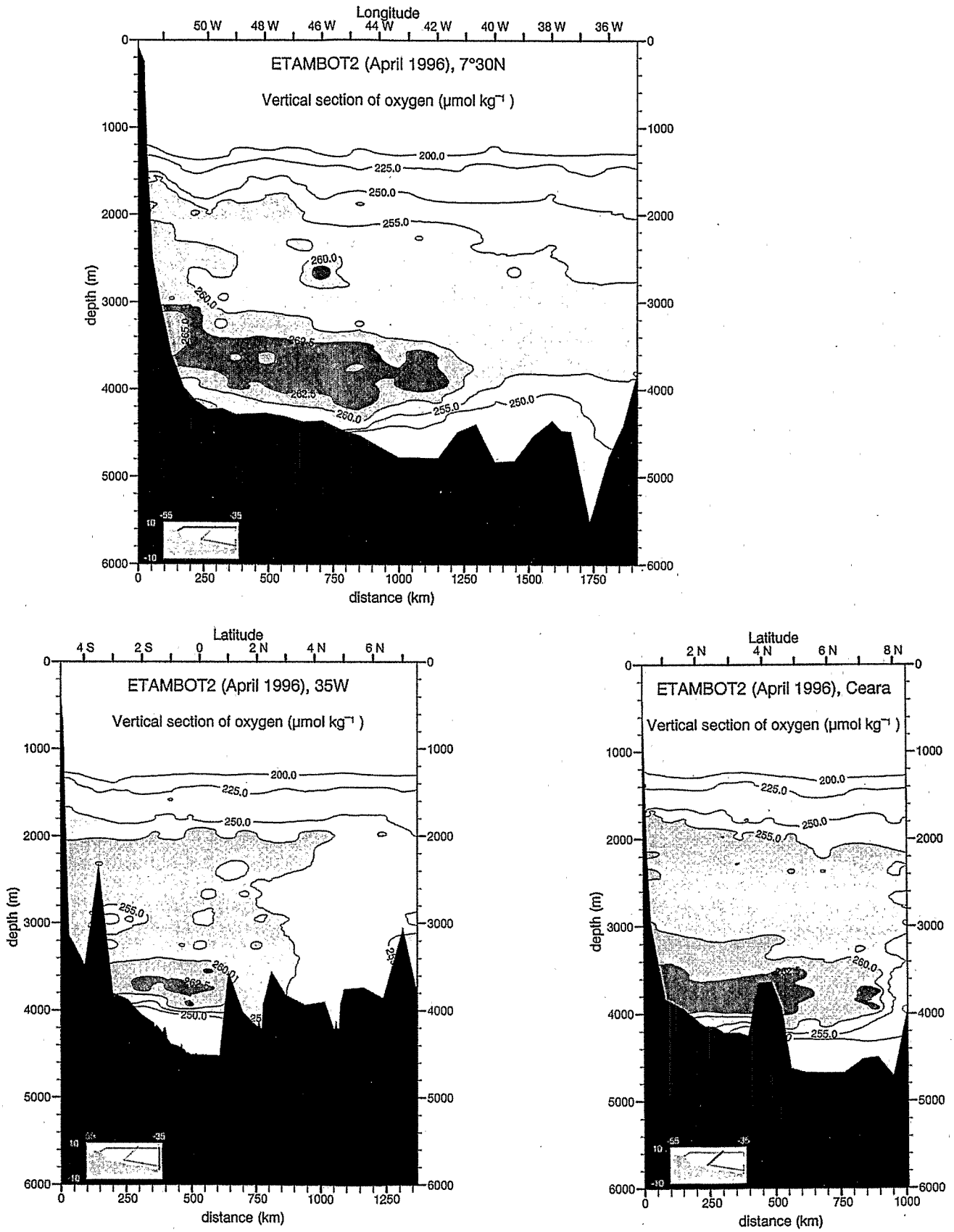

Figure 7. Vertical sections of dissolved oxygen (µmol kg^{-1}) obtained during ETAMBOT 2 in April-May 1996 along the (a) 7°30'N, (b) 35°W and (c) Ceara sections.

Rossby waves forced by the seasonally varying winds [*Böning and Schott*, 1993; *Li et al.*, 1996]. The observation of a more intense DWBC and its associated recirculation during ET2 (April 1996) than during ET1 (October 1995) is not sufficient to give any conclusive interpretation of such a possible seasonal variability.

5.2. Variability of the Zonal Circulation

Considerable spatiotemporal variability is observed on the 35°W section at the UNADW level. The ET2 pattern is very different from the usual pattern [*Rhein et al.*, 1995; 1998b; *Andrié et al.*, 1998]. This corresponds to the highly variable zonal circulation reported by *Richardson and Fratantoni* (1999) in the equatorial band (5°S-5°N). This variability may have several origins.

Some of these heterogeneous structures can be partly the result of the quasi-seasonal variability of the DWBC. The CFC core stuck on the continental slope near 5°S is not permanent. The core was not present during CIT1 (Figure 2b), was highest during ET1 (> 0.14 pmol kg^{-1}, Figure 3b), and nearly disappeared during ET2 (Figure 4b).

Others are linked to extraequatorial variability. A CFC enriched (and salty) core is observed north of 6°N during April 1996 (ET2). During CIT1 there is also a high salinity core, but it is less evident in CFC data. *Böning et al.* [1998] indicate, from the DYNAMO (DYnamics of the North Atlantic MOdeling) ocean general circulation model (OGCM) intercomparison, a seasonal variability in NADW transport around 1500 m depth. The model reproduces a direct seasonal input from the DWBC during summer. Off the equator, other thin, slice-like cores are observed all along the section, associated with salinity extremes, which could be related to different proportions of the MW component. *Curry et al.* [1998] describe an interannual variability of interactions between LSW and MW components within the UNADW. *Spall* [1996] gives importance to eddy-driven recirculation within the DWBC (within the Gulf Stream area as well as near the equator). Such interannual variabilities could be responsible for the prominent vertical and horizontal patch structure of the CFC distributions.

Finally, as observed within the DWBC at the 7°30'N section and upstream at higher latitudes [*Curry et al.*, 1998; *Pickart and Smethie*, 1998; *Molinari et al.*, 1998], a large-scale variability of the CFC distribution linked to the variability of the CFC input from the Nordic Seas is expected and seems to occur in 1996 through the large CFC signal observed at the LSW level.

Some other heterogeneities are attributable to the equatorial jets. These particular features are observed in the 2°S-2°N band. In the Atlantic, Gouriou et al. [this issue] describe a small, vertical-scale shear associated with the jets, superimposed on a large-scale vertical, linear shear. A reversal is observed for opposite seasons, maybe owing to the seasonal change of the thermocline depth in response to the wind variability. It is of interest to note that the CFC maximum observed at 1500 m on the ET2 35°W section at the equator (Figure 4b) coincides exactly with an eastward equatorial jet [*Gouriou et al.*, this issue]. The CFC minimum observed during ET1 at the equator around 1600 m can also correspond to a deep jet (Figure 3b). Such a variability could be linked to the reversal of equatorial deep jets [*Gouriou et al.*, this issue; *Richardson and Fratantoni*, 1999].

The question of the origin of the CFC tongue along the equatorial Atlantic has been addressed by *McCartney* [1993], *Kawase et al.* [1992], and *Böning and Schott* [1993] from numerical experiments. *Li et al* [1996] argue that Rossby waves play a dominant role in producing a chaotic stirring responsible for Lagrangian dispersion and tracer transport along the equator. V.Thierry et al. (Direct observations of low frequency fluctuations in the deep equatorial Atlantic ocean, submitted to *J. Geophys. Res.*, 1999) reproduce the annual and semiannual cycles of the UNADW and LNADW zonal flows measured across the Romanche and Chain Fracture Zones, from a sum of equatorial waves. They explain the eastward CFC core propagation by the Stokes drift due to the superimposition of the Rossby equatorially trapped waves rather than by a real eastward flow. Conversely, *Richardson and Fratantoni* [1999]

Table 2a. Evolution of CFC-11, Potential Temperature, Salinity, Oxygen, and Silicate Concentrations in the Upper North Atlantic Deep Water, 1993-1996.

	CITHER 1 March 1993	ETAMBOT 1 October 1995	ETAMBOT 2 April 1996
	7°30'N, West of 46°W		
CFC-11	0.234	0.299	0.298
Potential temperature	4.26	4.125	4.208
Salinity	35.007	35.000	35.002
Oxygen	245.3	245.5	242.2
Silicate	15.1	15.4	16.3
	Ceara		
CFC-11		0.136	0.167
Potential temperature		4.104	4.073
Salinity		34.972	34.987
Oxygen		233.8	241.2
Silicate		16.6	16.62
	35°W		
CFC-11	0.090	0.130	0.131
Potential temperature	4.024	3.991	3.971
Salinity	34.984	34.982	34.984
Oxygen	243.6	240.2	242.7
Silicate	17.55	16.9	17.0

Units are CFC-11, pmol kg^{-1}; potential temperature, °C ; salinity, psu ; oxygen, µmol kg^{-1}; and silicate, µmol kg^{-1}. Mean concentrations of samples were taken at 1600 m depth (no interpolation) for stations located to the west of 46°W, within the Deep Western Boundary Current.

Table 2b. Evolution of CFC-11, Potential Temperature, Salinity, Oxygen, and Silicate Concentrations in Labrador Sea Water, 1993-1996

	CITHER 1 March 1993	ETAMBOT 1 October 1995	ETAMBOT 2 April 1996
	7°30'N, West of 46°W		
CFC-11	0.068	0.131	0.164
Potential temperature	3.394	3.437	3.421
Salinity	34.980	34.980	34.980
Oxygen	259.9	256.7	257.5
Silicate	18.17	18.06	18.55
	Ceara		
CFC-11		0.101	0.091
Potential temperature		3.472	3.409
Salinity		34.978	34.975
Oxygen		253.8	255.9
Silicate		17.7	18.66
	35°W		
CFC-11	0.044	0.098	0.080
Potential temperature	3.370	3.453	3.452
Salinity	34.972	34.975	34.975
Oxygen	256.5	254	254.2
Silicate	20.18	18.6	18.81

Units are as in Table 2a. Mean concentrations of samples were taken at 2000 m depth.

Table 2c. Evolution of CFC-11, Potential Temperature, Salinity, Oxygen, and Silicate Concentrations in Middle North Atlantic Deep Water, 1993-1996

	CITHER 1 March 1993	ETAMBOT 1 October 1995	ETAMBOT 2 April 1996
	7°30'N, West of 46°W		
CFC-11	0.058	0.087	0.118
Potential temperature	2.393	2.457	2.447
Salinity	34.927	34.928	34.926
Oxygen	261.5	259.2	259.6
Silicate	30.24	29.0	30.1
	Ceara		
CFC-11		0.069	0.059
Potential temperature		2.510	2.499
Salinity		34.930	34.929
Oxygen		258.53	258.3
Silicate		27.8	28.72
	35°W		
CFC-11	0.020	0.031	0.016
Potential temperature	2.442	2.470	2.451
Salinity	34.924	34.923	34.922
Oxygen	258.1	255.4	254.9
Silicate	32.17	31.5	31.98

Units are as in Table 2a. Mean concentrations of samples were taken at 3000 m depth.

Table 2d. Evolution of CFC-11, Potential Temperature, Salinity, Oxygen, and Silicate Concentrations in Lower North Atlantic Deep Water, 1993-1996

	CITHER 1 March 1993	ETAMBOT 1 October 1995	ETAMBOT 2 April 1996
	7°30'N, West of 46°W		
CFC-11	0.099	0 .184	0.157
Potential temperature	2.003	1.994	1.976
Salinity	34.900	34.900	34.899
Oxygen	266.45	264.89	264.4
Silicate	32.96	31.9	33.67
	Ceara		
CFC-11		0.127	0.108
Potential temperature		2.008	2.023
Salinity		34.889	34.900
Oxygen		262.6	262.4
Silicate		33.1	33.29
	35°W (South)		
CFC-11	0.072	0.112	0.116
Potential temperature	2.026	1.951	2.002
Salinity	34.900	34.891	34.899
Oxygen	260.2	260.3	262.5
Silicate	34.7	34.7	33.6

Units are as in Table 2a. Mean concentrations of samples were taken at 3800 m depth. Only the stations sampled south of the equator are considered in the mean.

Table 2e. Evolution of CFC-11, Potential Temperature, Salinity, Oxygen, and Silicate Concentrations in Antarctic Bottom Water, 1993-1996

	CITHER 1 March 1993	ETAMBOT 1 October 1995	ETAMBOT 2 April 1996
	7°30'N, 40°W		
CFC-11	0.019	0.031	0.024
Potential temperature	1.191	1.193	1.221
Salinity	34.81	34.807	34.811
Oxygen	240.4	240.9	241.4
Silicate	74	76.4	81.6
	Ceara, 42°W		
CFC-11		0.025	0.021
Potential temperature		1.118	1.194
Salinity		34.798	34.808
Oxygen		239.7	240.7
Silicate		77	73.6
	35°W, 0°40'N		
CFC-11	0.016	0.017	0.007
Potential temperature	0.553	0.567	0.601
Salinity	34.74	34.738	34.739
Oxygen	225	227.2	226.3
Silicate	109.1	106.3	103.2

Units are as in Table 2a. Mean concentrations of samples were taken at the bottom.

argue for a real eastward water and tracer transport. The question of the origin of the CFC core and its link to the equatorial dynamics is still open.

5.3. Variability of the Mean NADW Characteristics

In order to observe the large-scale evolution of the characteristics of the western tropical Atlantic between 1993 and 1996, the mean concentrations of CFC-11, potential temperature, salinity, oxygen, and silicate within the DWBC core for the UNADW, LSW, MNADW, LNADW, and AABW levels for each section are given in Tables 2a-2e. For the 7°30'N section, only the area located between the American continental slope and 46°W is considered. The whole section is considered for the Ceara mean concentrations. Along the 35°W section the mean concentrations concern only the southern part of the equatorial channel, where the main part of the DWBC flow occurs (Figures 2b-2d and Plates 1a-1c). For simplicity and in order to avoid any interpolation, the means are calculated from data at common sampling depths, 1600 m for UNADW, 2000 m for LSW, 3000 m for MNADW, 3800 m for LNADW, and >4500 m for AABW.

At the UNADW level, along 7°30'N within the DWBC, CFC-11 concentration increases by 11% yr^{-1} between CIT1 and ET1 (Table 2a and Figure 8 left). This is in agreement with the annual increase in atmospheric concentration around the 1980s (S.Walker, personal communication, 1998). At 35°W (Figure 8 right), the annual increase is 17% yr^{-1} between CIT1 and ET1 as a result of a greater influence of local dynamics variability on the tracer fields. For the three sections the mean CFC concentrations do not considerably change between ET1 and ET2.

At the LSW level (Table 2b), CFC concentration increases considerably after CIT1. The annual increasing rates are 37% yr^{-1} between CIT1 and ET1 and 50% yr^{-1} between ET1 and ET2. This is surprising as LSW was described as a not recently ventilated water before 1993 within the tropics [*Molinari et al.*, 1992; *Rhein et al.*, 1995; *Andrié et al.*, 1998]. Further studies are in progress (C.Andrié et al., manuscript in preparation, 1999) in order to relate the sudden CFC increase and the greater vertical extent (down to 2400 m) that occurred in ET2 (Figure 4a)

At the MNADW level (Table 2c), the CFC-11 concentration increases from CIT1 to ET1 (20% yr^{-1}) and from ET1 to ET2 (71% yr^{-1}). Such CFC-11 increasing rates are probably due to a GFZW input within a CFC-devoid reservoir before 1993 [*Molinari et al.*, 1992]. This signal did not reach the Ceara and 35°W sections during 1996. The low silicate values (Table 2c) suggest that the greatest northern input occurs during ET1. Between 1993 and 1995-1996 the greatest CFC inputs from northern origin occur on both LSW and MNADW levels, probably from newly ventilated northern waters not identified before within the tropics but recently reported in the subtropics [*Molinari et al.*, 1998; *Pickart and Smethie*, 1998].

At the LNADW level we observe a 34% yr^{-1} CFC-11 increase between CIT1 and ET1 at 7°30'N associated with a silicate decrease (Table 2d and Figure 8). For the 7°30'N and Ceara sections there is a CFC-11 decrease between ET1 and ET2, associated with an oxygen decrease and a silicate increase. A somewhat different evolution of the LNADW characteristics is observed along 35°W, where the situation is reversed. There, higher CFC-11 and oxygen and lower silicate concentrations are observed during ET2 compared with ET1.

We interpret Figure 8 as a general evolution of the CFC mean concentrations within the DWBC. The effect of the atmospheric increase at the UNADW and LNADW levels is modulated by additional inputs from ventilated waters not present in the tropical area before 1993. Superimposed effects are linked to the variability of the circulation. From nontransient tracers (silica, oxygen, see Tables 2) it appears that the ET1 situation (October 1995) corresponds to the greatest southward flow over the whole deep water column, down to 4000 m.

Recently, several authors have pointed out evidence for a seasonal or semiannual cycle in transports of LNADW and AABW near the equator. From a mooring deployment around 35°W during 1993-1994, *Hall et al.* [1997] describe a boundary LNADW transport intensified during April-May and a minimum during the boreal fall. Conversely, the AABW transport is maximum in September-October and minimum in

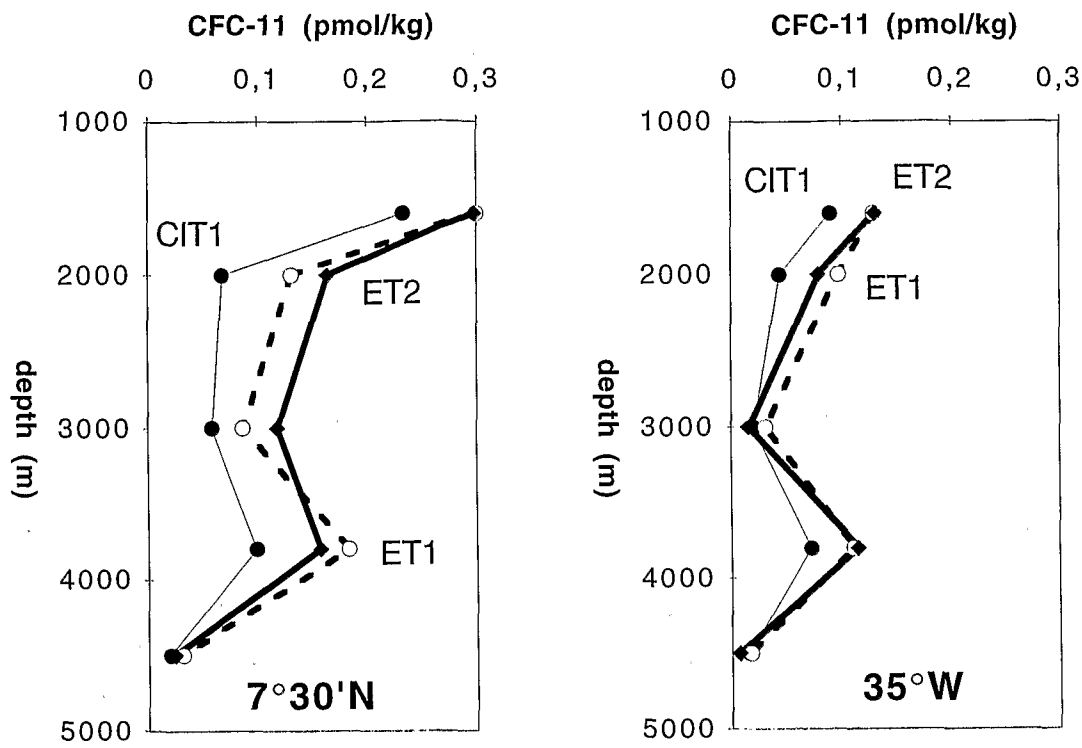

Figure 8. CFC-11 mean concentration profiles for the Deep Western Boundary Current along the (left) 7°30'N section and the (right) 35°W section for CIT1 (thin solid line), ET1 (dotted line), and ET2 (thick solid line) cruises. The mean values are from Table 2.

February-March. From combined LADCP and Pegasus measurements carried out along the 35°W meridian, *Fischer and Schott* [1997] observe strong LNADW eastward flow, between 1°S-2°S, in March-June. At 44°W, from mooring measurements, *Fischer and Schott* [1997] show that the DWBC transport (between 1000 and 3100 m) is minimum in September-October and maximum in January-February.

From hydrological and tracer characteristics we observe a greater southward flow during ET1 (October 1995) than CIT1 and ET2. This feature does not correspond to the situations of *Hall et al.* [1997] and *Fischer and Schott* [1997]. The high contrast observed in CFC and silicate concentrations at 35°W between ET1 and the two other cruises at the MNADW level (Table 2c) could also result from a stronger northward circulation of the southern waters, carrying more CFC-free waters, during CIT1 and ET2 compared with ET1. This circulation change could explain, at the LNADW level, the erosion of the upper part of the CFC core on the Ceara section during ET2 (Figure 4c).

Table 2e compares the AABW characteristics along the three sections. Potential temperature increases from CIT1 to ET2, associated with a silicate decrease (on 35°W and Ceara sections), which reflects a lower AABW influence during ET2 than ET1. It is difficult to determine the respective roles of seasonal or interannual variability in this evolution. The present results do not correspond to the *Hall et al.* [1997] observations, which argue for a simultaneous decrease of AABW influence and an increase in LNADW influence during boreal spring.

During ET1 the link between the maximum CFC-11 concentration and the maximum AABW input observed through silicate and temperature is not obvious to assess owing to experimental errors. A change of the AABW characteristics or a higher WSBW input could explain the associated high CFC-11 concentration within the equatorial channel during this cruise, suggesting some ventilated component arrival. During ET2 the low CFC signal (near detection limit) at the bottom indicates that no input from the ventilated WSBW waters has reached the tropics, in agreement with *Rhein et al.* [1998a]. The silicate section (Figure 6) shows that only the LCPW component of the AABW reached the tropical Atlantic in 1996.

These results rule out a dominant seasonal variability of the deep circulation during the 1993-1996 time interval. During this period there must be an interannual deep circulation variability affecting either the direct southward flow or the recirculation or intrusion of waters from southern origin. A great deal of work is still required on this topic, including analysis of more complete series from different data sets.

Acknowledgments. We are particularly grateful to the captains and crews of the R/V *Le Noroît* and the R/V *Edwin Link* , who have made possible all the measurements under very good onboard conditions. We thank W. Biegun, who helped in CFC analysis during ETAMBOT 2 and P. Laberiotte for data processing. This work was supported by Institut de Recherche pour le Développement (IRD, formerly ORSTOM) as part of the Programme National d'Etude de la Dynamique du Climat (PNEDC) and its WOCE/France subprogramme.

References

Andrié, C., Chlorofluoromethanes in the deep equatorial Atlantic revisited, in *The South Atlantic: Present and Past Circulations*, edited by G.Wefer et al., pp. 273-288, Springer-Verlag, New-York, 1996.

Andrié, C., Y. Gouriou, B. Bourlès, C. Oudot, and J.F. Temon, Deep circulation in the Western Tropical Atlantic inferred from CFCs and L-ADCP Measurements during ETAMBOT cruises, *Int. WOCE*

Newsl., vols 28 and 29, Int. Proj. Off., Southampton Oceanogr. Cent., Southampton, England, October 1997.

Andrié, C., J.F. Ternon, M.J. Messias, L. Memery, and B. Bourlès, Chlorofluoromethanes distributions in the deep equatorial Atlantic during January-March 1993, *Deep Sea Res., Part I, 45*, 903-930, 1998.

Arhan, M., H. Mercier, B. Bourlès, and Y. Gouriou, Two hydrographic sections across the Atlantic at 7°30'N and 4°30S, *Deep Sea Res., Part I, 45*, 829-872, 1998.

Böning, C., and F. Schott, Deep currents and the eastward salinity ton-gue in the equatorial Atlantic: results from an eddy-resolving, pri-mitive equation model, *J. Geophys. Res., 98*, 6991-6999, 1993.

Böning, C., C. Dieterich, Y. Jia, and B. Barnier, Seasonal variability of deep currents in the equatorial Atlantic: results from the DYNAMO project (abstract), *Ann. Geophys., 16*, (II), C538, 1998.

Bönisch, G., J. Blindheim, J. Bullister, P. Schlosser, and D.W.R. Wallace, Long-term trends of temperature, salinity, density, and transient tracers in the central Greenland Sea, *J. Geophys. Res., 102*, 18,553-18,571, 1997.

Bourlès B., Y. Gouriou, and R. Chuchla, On the circulation in the upper layer of the western equatorial Atlantic, *J. Geophys. Res.*, this issue.

Bullister, J.L., and R.F. Weiss, Determination of CCl_3F and CCl_2F_2 in seawater and air, *Deep Sea Res., Part A, 35*, 839-853, 1988.

Colin, C., B. Bourlès, R. Chuchla, and F. Dangu, Western boundary current variability off French Guiana as observed from moored current measurements, *Oceanol. Acta, 17*, 345-354, 1994.

Curry, R.G., M.S. McCartney, and T.M. Joyce, Oceanic transport of subpolar climate signals to mid-depth subtropical waters, *Nature, 391*, 575-577, 1998.

Dickson, R., From the Labrador Sea to global change, *Nature, 386*, 649-650, 1997.

Dickson, R.R., E.M. Gmitrowitz, and A.L. Watson, Deep water renewal in the north Atlantic, *Nature, 344*, 848-850, 1990.

Döscher, R., and R. Redler, The relative importance of northern overflow and subpolar deep convection for the North Atlantic Thermohaline circulation, *J. Phys. Oceanogr., 27*, 1894-1902, 1997.

Equipe ETAMBOT, Recueil de données, Campagne ETAMBOT 1, N.O. Le Noroit (9 septembre - 11 octobre 1995), vols 1 and 2, *Doc. Sci. 22 and 23*, Cent. ORSTOM, Cayenne, French Guiana, 1997a.

Equipe ETAMBOT, Recueil de données, Campagne ETAMBOT 2, N.O. Edwin Link (12 avril - 16 mai 1996), vols 1 and 2, *Doc. Sci. 24 and 25*, Cent. ORSTOM, Cayenne, French Guiana, 1997b.

Fine, R.A., and R.L. Molinari, A continuous deep western boundary current between Abaco (26,5°N) and Barbados (13°N), *Deep Sea Res., Part A, 35*, 1441-1450, 1988.

Fischer, J., and F. A. Schott, Seasonal transport variability of the Deep Western Boundary Current in the equatorial Atlantic, *J. Geophys. Res., 102*, 27,751-27,769, 1997.

Friedrichs, M.A., and M.M. Hall, Deep circulation in the tropical North Atlantic, *J. Mar. Res., 51*, 697-736, 1993.

Friedrichs, M.A., M.S. McCartney, and M.M. Hall, Hemispheric asymmetry of deep water transport modes in the western Atlantic, *J. Geophys. Res., 99*, 25,165-25,179, 1994.

Gouriou, Y., B. Bourlès, H. Mercier, and R. Chuchla, Deep jets in the equatorial Atlantic Ocean, *J. Geophys. Res.*, this issue.

Groupe CITHER 1, Recueil de données, campagne CITHER 1, N.O. L'Atalante (2 janvier-19 mars 1993), vol. 2, CTD-O_2. *Rap. LPO 94-04*, 499 pp., Laboratoire de Physique des Océans, Brest, France, 1994.

Hall, M.M., M. McCartney, and J.A. Whitehead, Antarctic Bottom Water flux in the equatorial western Atlantic, *J. Phys. Oceanogr., 27*, 1903-1926, 1997.

Johns, W.E., D.M. Fratantoni, and R. Zantopp, Deep western boundary current variability off northeastern Brazil, *Deep Sea Res., Part I, 40*, 2, 293-310, 1993.

Kawase, M., L.M. Rothstein, and S.R. Springer, Encounter of a Deep Western Boundary Current with the equator: A numerical spin-up experiment, *J. Geophys. Res., 97*, 5447-5463, 1992.

Lazier, J.R.N., Temperature and salinity changes in the deep Labrador sea, 1962-1986, *Deep Sea Res., Part A, 35*, 1247-1253, 1988.

Lee, T.N., W.E. Johns, R.J. Zantopp, and E.R. Fillenbaum, Moored observations of Western Boundary Current variability and thermaohaline circulation at 26.5°N in the Subtropical North Atlantic, *J. Phys. Oceanogr., 26*, 962-983, 1996.

Li, X., P. Chang, and R.C. Pacanowski, A wave-induced stirring mechanism in the mid-depth equatorial ocean, *J. Mar. Res., 54*, 487-520, 1996.

Mauritzen, C., Production of dense overflow waters feeding the North Atlantic across the Greenland-Scotland Ridge, 1, Evidence for a revised circulation scheme, *Deep Sea Res., Part I, 43*, 769-806, 1996.

McCartney, M.S., Crossing of the equator by the Deep Western Boundary Current in the Western Atlantic Ocean, *J. Phys. Oceanogr., 23*, 1953-1974, 1993.

Mercier, H., K.G. Speer, and J. Honnorez, Flow pathways of bottom water through the Romanche and Chain fracture zones, *Deep Sea Res., Part I, 41*, 1457-1477, 1994.

Messias, M.J., C. Andrié, L. Memery, and H. Mercier, Tracing the North Atlantic Deep Water through the Romanche and Chain fracture zones using chlorofluoromethanes, *Deep Sea Res., Part I*, in press, 1999.

Molinari, R.L., R.A. Fine, and E. Johns, The Deep Western Boundary Current in the tropical North Atlantic Ocean, *Deep Sea Res., Part A, 39*, 1967-1984, 1992.

Molinari, R.L., R.A. Fine, W.D. Wilson, R. Curry, J. Abell, and M.McCartney, The arrival of recently formed Labrador Sea Water in the deep western boundary current at 26.5°N, *Geophys. Res. Lett., 25*, 2249-2252, 1998.

Oudot, C., P. Morin, F. Baurand, M. Wafar and P. Le Corre, Northern and southern water masses in the equatorial Atlantic sector: Results of nutrients from CITHER1 cruise (WOCE A6 and A7 lines), *Deep Sea Res., Part I, 45*, 873-902, 1998.

Oudot, C., J.F. Ternon, C. Andrié, E.S. Braga, and P. Morin, On the crossing of the equator by intermediate water masses in the western Atlantic Ocean: Identification and pathways of Antarctic Intermediate Water and Upper Circumpolar Water, *J. Geophys. Res.*, this issue.

Pickart, R.S., Water mass components of the North Atlantic deep western boundary current, *Deep Sea Res., Part A, 39*, 1553-1572, 1992.

Pickart, R.S., and W.M. Smethie Jr., Temporal evolution of the deep western boundary current where it enters the sub-tropical domain, *Deep Sea Res., Part. I, 45*, 1053-1083, 1998.

Pickart, R.S., W.M. Smethie Jr., J.R.N. Lazier, E.P. Jones, and W.J. Jenkins, Eddies of newly formed upper Labrador Sea water, *J. Geophys. Res.*, 101, 20,711-20,726, 1996.

Pickart, R.S., M.A. Spall, and J.R.N. Lazier, Mid-depth ventilation in the western boundary current system of the sub-polar gyre, *Deep-Sea Res., Part I, 44*, 1025-1054, 1997.

Plähn, O., and M. Rhein, Measured and modeled CFC distribution of lower NADW in the Guiana Basin, *J. Geophys. Res., 103*, 2831-2847, 1998.

Reid, J.L., On the total geostrophic calculation of the North Atlantic ocean: flow patterns, tracers, and transports, *Prog. Oceanogr., 33*, 1-92, 1994.

Rhein, M., Ventilation rates of the Greenland and Norwegian Seas derived from distributions of the chlorofluoromethanes F-11 and F-12, *Deep Sea Res., Part A, 38*, 485-503, 1991.

Rhein, M., Convection in the Greenland Sea, 1982-1993, *J. Geophys. Res., 101*, 18,183-18,192, 1996.

Rhein, M., L. Stramma, and U. Send, The Atlantic Deep Western Boundary Current: Water masses and transports near the equator, *J. Geophys.Res., 100*, 2441-2457, 1995.

Rhein, M., L. Stramma, and G. Krahmann, The spreading of Antarctic Bottom Water in the tropical Atlantic, *Deep Sea Res., Part I, 45*, 507-527, 1998a.

Rhein, M., O. Plähn, R. Bayer, L. Stramma, and M. Arnold, Temporal evolution of the tracer signal in the Deep Western Boundary Current, tropical Atlantic, *J. Geophys. Res., 103*, 15,869-15,883, 1998b.

Richardson, P.L., and D.M. Fratantoni, Float trajectories in the Deep Western Boundary Current and deep equatorial jets of the tropical Atlantic, *Deep-Sea Res., Part II, 46*, 305-333, 1999.

Richardson, P.L., and W.J. Schmitz Jr., Deep cross-equatorial flow in the Atlantic measured with SOFAR floats, *J. Geophys. Res., 98*, 8371-8387, 1993.

Schott, F., J. Fischer, J. Reppin, and U. Send, On mean and seasonal currents and transports at the western boundary of the equatorial Atlantic, *J. Geophys. Res., 98*, 14,353-14,368, 1993.

Schlosser, P., G. Bonisch, M. Rhein, and R. Bayer, Reduction of

deepwater formation in the Greenland sea during the 1980s: Evidence from tracer data, *Science, 251*, 1054-1056, 1991.

Smethie, W.M., Jr., Tracing the thermohaline circulation in the western North Atlantic using chlorofluorocarbons, *Prog. Oceanogr., 31*, 51-99, 1993.

Smethie, W.M., H.G. Ostlund, and H.H. Loosli, Ventilation of the deep Greenland and Norwegian seas: Evidence from krypton-85, tritium, carbon-14 and argon-39, *Deep Sea Res., Part A, 33*, 675-703, 1986.

Spall, M., Dynamics of the Gulf Sream/Deep Western Boundary Current Crossover, I, Entrainement and recirculation, *J. Phys. Oceanogr., 26*, 2152-2168, 1996.

Speer, K.G., and M.S. McCartney, Tracing lower north Atlantic deep water across the equator, *J. Geophys. Res., 96*, 20,443-20,448, 1991.

Sy, A., M. Rhein, J.R.N. Lazier, K.P. Koltermann, J. Meinke, A. Putska, and M. Bersch, Surprisingly rapid spreading of newly formed intermediate waters across the North Atlantic Ocean, *Nature, 386*, 675-679, 1997.

Talley, L.D., and G.C. Johnson, Deep, zonal subequatorial currents, *Science, 263*, 1125-1128, 1994.

Vaughan, S.L., and R.L. Molinari, Temperature and salinity variability in the Deep Western Boundary Current, *J. Phys. Oceanogr., 27*, 749-761, 1997.

Warner, M.J., and R.F. Weiss, Solubilities of chlorofluorocarbons 11 and 12 in water and seawater, *Deep Sea Res., Part A, 32*,1485-1497, 1985.

Weiss, R.F., J.L. Bullister, R.H. Gammon, and M.J. Warner, Atmospheric chlorofluoromethanes in the deep equatorial Atlantic, *Nature, 314*, 608-610, 1985.

C. Andrié, Laboratoire d'Océanographie Dynamique et de Climatologie, CNRS/IRD/ Univesité Pierre et Marie Curie, 4 place Jussieu, case 100, 75252 Paris Cedex 05, France. (andrie@lodyc.jussieu.fr)

B. Bourlès, Y. Gouriou and C. Oudot, Institut de Recherche pour le Développement, BP70, 29180, Plouzané, France. (bbourles@ifremer.fr; ygouriou@ifremer.fr; coudot@ifremer.fr)

J. F. Ternon, Institut de Recherche pour le Développement, BP 165 Cayenne, French Guiana. (ternon@cayenne.ird.fr)

(Received April 28, 1998 ; revised January 28, 1999; accepted March 26, 1999.)